ELUCIDATING SYNERGISTIC INTERACTIONS IN MICROBIAL COMMUNITIES CONSISTING OF COMPLEMENTARY *E. COLI* AUXOTROPHS

by

Ryan A. McNulty

A thesis submitted to the Faculty of the University of Delaware in partial fulfillment of the requirements for the degree of Honors Bachelor in Chemical Engineering with Distinction

Spring 2018

ELUCIDATING SYNERGISTIC INTERACTIONS

IN MICROBIAL COMMUNITIES CONSISTING OF

COMPLEMENTARY *E. COLI* AUXOTROPHS

by

Ryan A. McNulty

Approved: _____

Maciek R. Antoniewicz, Ph.D.
Professor in charge of thesis on behalf of the Advisory Committee

Approved: _____

Eleftherios T. Papoutsakis, Ph.D.
Committee member from the Department of Chemical and Biomolecular Engineering

Approved: _____

Christopher J. Kloxin, Ph.D.
Committee member from the Board of Senior Thesis Readers

Approved: _____

Paul Laux, Ph.D.
Director, University Honors Program

ACKNOWLEDGMENTS

First and foremost, I would like to thank my parents, Mark and Cathleen. You have enabled everything I've done in life and I am forever grateful for your unwavering love and support. In pursuing all of my interests, including academic research, I strive to make you proud every day.

Second, I must thank Dr. Maciek Antoniewicz, my research advisor. Your willingness to let me join your research group and dive into this exciting and novel project meant the world to me as a young undergraduate looking to find a place within academia. Since then, you have tirelessly guided me through this work while patiently teaching me the concepts and procedures behind metabolic engineering. Altogether, your training and promotion for autonomy within the lab has allowed me to develop as both a researcher and student by encouraging critical thinking.

Next, I thank all of my friends and peers who supported my research endeavors and motivated me to complete a senior thesis. Specifically, I would like to extend my sincerest gratitude to Nikodimos Gebreselassie for introducing me into the laboratory and taking time out of your schedule as a graduate student to teach me the various experiments and techniques required by this project.

Lastly, I am grateful to the University of Delaware for giving me the opportunity to perform undergraduate research and challenging me to strive for an Honors Degree with Distinction. I would also like to thank the rest of my thesis committee, Dr. Eleftherios (Terry) Papoutsakis and Dr. Christopher J. Kloxin, for their assistance in reviewing and providing feedback on my research.

Ryan McNulty

Spring 2018

TABLE OF CONTENTS

LIST OF TABLES

LIST OF FIGURES

ABSTRACT

In nature, microorganisms can exist in diverse, integrated communities wherein metabolic intermediates, in addition to substrates and products, are shared synergistically to enable biochemical phenotypes unobserved in clonal monocultures. In this work, co-cultures of complementary *Escherichia coli* auxotrophs are studied through ^{13}C metabolic flux analysis (^{13}C-MFA) to elucidate the cooperative interactions between strains. Co-culture models outlining the central carbon metabolism reaction network of each strain as well as the exchange reactions between species within a co-culture were developed and fit to isotopomer distributions obtained through ^{13}C labeled glucose tracer experiments to identify cross-fed metabolites and estimate metabolic fluxes. In a preliminary analysis, isoleucine and α-ketoglutarate were identified as two metabolites likely to be exchanged within a co-culture consisting of two auxotrophic *E. coli* strains with icd and ilvC knockouts, respectively, while alanine and α-ketoglutarate were identified for a co-culture consisting of Δicd and ΔargE mutants. In addition, amino acid supplemented agar plating assays were utilized to reveal feedback controlled growth dynamics that follow mutualism by *invested benefits*. Furthermore, experiments with Transwell® permeable supports reveal the employment of an efficient exchange mechanism in which metabolites are shared by secretion into the cell medium. Adaptive laboratory evolution experiments demonstrated the ability for this mechanism to be improved with a 56% increase in the growth rate of the Δicd/ΔilvC co-culture (from 0.170 h^{-1} to 0.265 h^{-1}) over 38 subcultures. Lastly, more complex metabolic models for the co-culture of Δicd and ΔilvC were developed to test current hypotheses regarding metabolite exchange. Through ^{13}C-MFA, a model predicting the exchange of amino acids between strains

was developed which obtained flux estimates with SSRs that fell near the 95% acceptable confidence level. With further tuning, we believe this model can accurately estimate central carbon metabolism and exchange fluxes for co-cultures of conditionally lethal *E. coli* mutants.

Chapter 1

INTRODUCTION

1.1 Motivations

Ubiquitous in nature, microbial communities can exert metabolic interactions that significantly alter the biochemical phenotypes of the involved species. In some cases, the integration of multiple metabolic networks in a collaborative multi-organism system can lead to improved metabolic efficiency such as an increased substrate uptake rate and/or greater product conversions.[1] These enhanced characteristics of microbial communities, compared to a collection of the characteristics offered by monocultures of the participating species, enforce the expression "the whole is greater than the sum of its parts" and can go forth to benefit a variety of industrial practices such as the production of biofuels and the breakdown of organic waste product.[2,3] Other advantageous traits observed in microbial communities relate to the fitness of comprising species, including an increased ability to adapt to environmental fluctuations and, in some cases, the ability to overcome auxotrophy.[4] Overall, multi-microorganism systems as simple as co-cultures (two species) can overcome many of the limitations faced in single-species systems.

---

[1] Sabra, W., Dietz, D., Tjahjasari, D., Zeng, A.P. (2010). Biosystems analysis and engineering of microbial consortia for industrial biotechnology. Eng. Life Sci. 10, 407–421.

[2] Bagi, Z., Acs, N., Bálint, B., Horváth, L., Dobó, K., Perei, K.R., Rákhely, G., Kovács, K.L. (2007). Biotechnological intensification of biogas production. Appl. Microbiol. Biotechnol. 76, 473–482.

[3] Gilbert, E.S., Walker, A.W., Keasling, J.D. (2003). A constructed microbial consortium for biodegradation of the organophosphorus insecticide parathion. Appl. Microbiol. Biotechnol. 61, 77–81.

Examples of communal microbial systems that exert altered, cooperative phenotypes include co-cultures of certain auxotrophic *Escherichia coli* mutants. While unable to grow on glucose in minimal media, specific combinations of auxotrophic strains have been demonstrated to grow as co-cultures under the same conditions.[4] With recent advances in metabolic flux analysis (MFA) techniques, species-specific fluxes within these co-cultures can be determined through isotopic labeling of biomass components without physical separation of cells or proteins.[5] In addition, the mechanisms through which metabolites are exchanged between species and the respective exchange fluxes can be elucidated. Ultimately, these methods are applied to quantify the metabolic interactions between microbial communities, therefore, providing insight and understanding as to how these multi-microorganism systems function and can be engineered to optimize industrial processes.

1.2 Thesis Aim

The aim of this research is to characterize the metabolic interactions occurring within specific co-cultures of complementary *E. coli* auxotrophs. This thesis seeks to identify all key metabolites exchanged between these complementary strains as well as the mechanisms through which this exchange occurs. To understand and quantify the reaction networks at play, metabolic models were developed and verified with ^{13}C metabolic flux analyses which were performed on monocultures of specific *E. coli* strains as well as on co-cultures of complementary pairs. Amino acid supplemented

---

[4] Wintermute, E.H., Silver, P.A. (2010). Emergent cooperation in microbial metabolism. Mol. Syst. Biol. 6, 407.

[5] Gebreselassie, N.A., Antoniewicz, M.R. (2015). (13)C-metabolic flux analysis of co-cultures: A novel approach. Metab. Eng. 31, 132-139.

plating assays were utilized to verify co-culture composition and differentiate between complementary strains while ratio tests captured population dynamics. Experiments with Transwell® membrane plates provided insight on the mass transport mechanism behind metabolite exchange. This work is the first extensive study utilizing ^{13}C metabolic flux analysis to analyze metabolite exchange within co-cultures.

Chapter 2

BACKGROUND

2.1 Co-cultures of *E. coli* Auxotrophs

Induced growth of auxotrophic *E. coli* mutants in minimal media through co-culture with complementary strains was first demonstrated by Wintermute and Silver in 2010.[4] Coining the observed synergistic interaction as "synthetic mutualism in trans", or SMIT, the study went forth to identify 176 co-cultures that exhibited SMIT, derived from different pairings of 46 conditionally lethal auxotrophic *E. coli* from the Keio collection.[6] Our study selected 11 of these mutants to produce 18 unique co-cultures - the observed growth results compared to those of the 2010 publication (see text for further details). The 11 selected, genetically-engineered strains represent a wide range of genetic diversity by including knockouts of genes required for the synthesis of amino acids as well as genes involved in central carbon metabolism. It has been proposed that successful co-cultures of the kind discussed in this study exist due to byproduct cooperation, where one strain of a complementary set secretes a waste product of limited value to itself but highly valued by the other strain. This type of syntrophic system is common in nature as it minimizes the integration of metabolic networks, arising more so out of natural convenience than evolved investment. In addition, an interdependent community of auxotrophic species can result in a more stable microbial system compared to prototrophic wild-type cells as metabolic labor is

---

[6] Baba, T., Ara, T., Hasegawa, M., Takai, Y., Okumura, Y., Baba, M., Datsenko, K.A., Tomita, M., Wanner, B.L., Mori, H. (2006). Construction of Escherichia coli K-12 in-frame, single-gene knockout mutants: the Keio collection. Mol. Sys. Bio. 2, 1-11.

divided to minimize the fitness costs associated with producing key metabolites.[7,8] While metabolites fitting the description for byproduct cooperation within specific co-cultures of auxotrophic *E. coli* strains have been predicted through joint stoichiometric & shadowing models[4], to the best of our knowledge, no study has utilized ^{13}C metabolic flux analysis to identify the metabolites contributing directly to SMIT.

2.2 ^{13}C-Metabolic Flux Analysis

Metabolic Flux Analysis (MFA) is a collection of techniques that quantifies the highly-regulated movement of matter through a cell's metabolic network. The flux of metabolites through each biochemical reaction associated with a cell's metabolism is defined as the rate of the forward reaction minus that of the reverse reaction. Overall, MFA describes the conversional flows of substrates into metabolic intermediates and products that, ultimately, provide the energy required to sustain cell life. Through MFA and the comparison of flux profiles across genetically diverse microorganisms, changes in intracellular fluxes, specifically in the central metabolism, can be tracked to elucidate differences in physiological states.

^{13}C-Metabolic Flux Analysis (^{13}C-MFA) is an experimental method that utilizes ^{13}C labeled substrates, typically ^{13}C-glucose, to determine the intracellular fluxes through major metabolic pathways within a specific microorganism. As a cell uptakes and metabolizes the substrate, the labeled carbon is incorporated into the

---

[7] Zengler, K., & Zaramela, L. S. (2018). The social network of microorganisms — how auxotrophies shape complex communities. *Nature Reviews Microbiology*.

[8] Pande, S., et al. (2013) Fitness and stability of obligate cross-feeding interactions that emerge upon gene loss in bacteria. ISME J. 8, 953-962.

various metabolites of its central metabolism. The distribution of ^{13}C in an organism's metabolic network at mid-log phase can then be used to estimate metabolic flux at steady state through the existence of isotopic isomers (isotopomers) – measured by the analytical methods of gas chromatography mass spectrometry (GC-MS) or nuclear magnetic resonance (NMR). Fitting these isotopomer distributions to stoichiometric balances of metabolites (more specifically, their carbon atoms) within a known metabolic network, thus, generates a flux profile which describes a cell's metabolic state *in vivo*. Currently, one of the most accurate models for estimating metabolic flux with isotopomer data utilizes the elementary metabolite unit (EMU) framework developed by Antoniewicz et al.[9] In short, the EMU framework utilizes specific combinations or "subsets" of a metabolite's atoms to track the atomic transitions occurring within a metabolic reaction network. A system of equations can then be generated that relates fluxes to stable isotope measurements and solved through a highly efficient decomposition algorithm.

[9] Antoniewicz, M.R., Kelleher, J.K., Stephanopoulos, G. (2007). Elementary metabolite units (EMU): a novel framework for modeling isotopic distributions. Metab. Eng. 9, 68–86.

Chapter 3

METHODOLOGY

3.1 Materials

Chemicals and media were purchased from Sigma-Aldrich (St. Louis, MO). Isotopic glucose tracers ([1,2-^{13}C], [1,6-^{13}C], [4,5,6-^{13}C], [U-^{13}C]) were purchased from Cambridge Isotope Laboratories. Glucose stock solutions (20% by weight) and kanamycin monosulfate stock solutions (1000x – 50 mg/mL) were prepared with distilled water. Stock solutions of amino acids (30 mM) were prepared by mixing the appropriate amount of amino acid powder with 50 mL of distilled water. All solutions were sterilized by filtration.

For *Escherichia Coli* cultures, minimal (M9) media was composed of the following materials (per L of media): 11.2 g M9 powder, 2 mL of 1 M MgSO4, and 100 µL of 1 M $CaCl_2$. Rich (LB) medium was prepared by mixing 12.5 g of LB power with 500 mL of distilled water and autoclaved. For both types of medium, glucose and kanamycin were then added as indicated.

Minimal (M9) agar plates were created in batches of 15 by evenly distributing autoclaved solutions of the following composition into sterile, Fisherbrand polystyrene petri dishes: 300 mL of H_2O, 3.36 g M9 power, 600 µL of 1 M MgSO4, 30 µL of 1 M $CaCl_2$, 4.5 g of agar, 3 mL of glucose (20% by weight), and 600 µL of kanamycin. Plates supplemented with specific amino acids were composed of the same bulk solution plus 10 mL of the respective 30 mM amino acid solution. Rich (LB) agar plates contained 300 mL of water, 12 g of LB agar powder, and 600 µL of kanamycin – mixed and autoclaved.

3.2 Strain and Growth Conditions

Eleven kanamycin resistant *E. coli* knockout strains from the Keio Knockout Collection were used in this study, tabulated below. The strains were purchased from GE Life Sciences/Dharmacon (Pittsburgh, PA). Co-culture experiments were performed under aerobic growth conditions at 37^{o}C in mini-bioreactors; either with a working volume of 4 mL (polystyrene test tubes) or a working volume of 10mL (Erlenmeyer flasks). All bioreactors were capped with foam-tube Identi-Plugs® (Jaece Industries) and shaken continuously at 225 rpm. To generate co-cultures, *E. coli* knockout strains were first pre-cultured individually under the same conditions until mid-exponential growth phase either in rich (LB) medium or minimal (M9) medium supplemented with the necessary amino acid supplements for growth. The initial glucose concentration in each bioreactor was approximately 2 g/L. To prevent contamination, kanamycin monosulfate was added to each culture at an initial concentration of 0.1 g/L. All bioreactors were autoclaved before inoculation.

Table 3.2.1. List of conditionally lethal *E. coli* mutants from the Keio Collection.

Strain	*ID*	*Description*
Δ*argE*	JW3929	Escherichia coli K-12 with deletion of argE gene
Δ*cysC*	JW2720	Escherichia coli K-12 with deletion of cysC gene
Δ*icd*	JW1122	Escherichia coli K-12 with deletion of icd gene
Δ*ilvC*	JW3747	Escherichia coli K-12 with deletion of ilvC gene
Δ*ilvE*	JW5606	Escherichia coli K-12 with deletion of ilvE gene
Δ*metA*	JW3973	Escherichia coli K-12 with deletion of metA gene
Δ*nadC*	JW0105	Escherichia coli K-12 with deletion of nadC gene
Δ*panD*	JW0127	Escherichia coli K-12 with deletion of panD gene
Δ*ppc*	JW3928	Escherichia coli K-12 with deletion of ppc gene
Δ*ptsI*	JW2409	Escherichia coli K-12 with deletion of ptsI gene
Δ*trpE*	JW1256	Escherichia coli K-12 with deletion of trpE gene

3.3 Mass Transport Experiment

Transwell® 24mm polycarbonate membrane cell culture inserts (product no. 3412) from Corning Life Sciences (Kennebunk, ME) were selected to study the mechanism of metabolite exchange within *E. coli* co-cultures. Each plate contained 6 wells (medium working volume of 2.5 mL) and 6 inserts (medium working volume of 1.5 mL) to allow six co-cultures to be grown in parallel. Each well and insert set was separated by a 10 μm thick polycarbonate membrane with pore sizes of 0.4 μm. Nominal pore density was 10^8 pores per square centimeter. To mitigate oxygen transfer limitations, the inoculated plates were shaken continuously at 200 rpm in a 37°C incubator. All plates were sterilized with gamma radiation by the manufacturer.

3.4 Tracer Experiments

3.4.1 *E. coli* Monocultures

For parallel ^{13}C labeling experiments of auxotrophic *E. coli* mono-cultures, cells from -80°C frozen stock were precultured in 10 mL of rich (LB) media (with kanamycin). Once the cells reached stationary phase (OD_{600} of ~1.5), 100 μL samples were subcultured into 10 mL of minimal media with 100 μL unlabeled glucose stock (20% by weight), 20 μL of kanamycin (50 mg/mL) and the appropriate amino acids at 1 mM final concentration (i.e. 333 μL of 30 mM stock solutions) to enable growth. Once cultures were fully grown, this subculture process was repeated once more. Upon reaching stationary phase in the second subculture, 100 μL of inoculum were transferred into 10 mL of fresh medium (M9, kanamycin, amino acid supplements) with 100 μL of a ^{13}C labeled carbon source - either [1,2-^{13}C], [1,6-^{13}C], or [U-^{13}C] glucose. To note, an additional 100 μL of unlabeled glucose were added to the cultures utilizing [U-^{13}C] glucose tracer. Cell densities of these cultures were measured

periodically over the course of 6 to 8 hours. Monoculture samples of labeled cell biomass were collected at an OD_{600} between 0.5 and 1.0 and centrifuged for 5 min at 14,000 rpm. The resulting cell pellet and supernatant were separated and stored at -20^{o}C for later analysis.

3.4.2 *E. coli* Co-cultures in Mini-Bioreactors

For parallel ^{13}C labeling experiments of *E. coli* co-cultures grown in a single, mini-bioreactor, a similar procedure as the one described above was followed, however, precultures were inoculated with two strains of *E. coli* in 10 mL of minimal media with 100 µL of unlabeled glucose and 20 µL of kanamycin. After reaching stationary phase (OD_{600} of ~1.5), 200 µL of inoculum from these cultures were transferred into fresh M9 media with kanamycin and 100 µL of labeled glucose tracer (either [1,2-^{13}C] or [1,6-^{13}C] glucose). Cell biomass was measured periodically over the next 12 hours; samples were collected, centrifuged, separated, and stored once the co-cultures reached an OD_{600} of 0.5.

3.4.3 *E. coli* Co-cultures in Permeable Supports

For parallel ^{13}C labeling experiments of *E. coli* co-cultures grown in Transwell permeable supports, individual strains of *E. coli* auxotrophs were first precultured in 5mL of minimal media with 50 µL of unlabeled glucose stock (20% by weight), 10 µL of kanamycin (50 mg/mL), and the necessary amino acids (at 1 mM concentrations) to enable growth. 4 mL aliquots of the grown cultures were then centrifuged and the cells washed with the necessary amount of minimal media to produce solutions with an OD_{600} of 4.0. 200 µL of these concentrated cultures were then used to inoculate either the inner well (working volume of 1.5 mL) or outer well (working volume of 2.5 mL)

of a Transwell support which contained the appropriate amount of minimal (M9) media with 20 µL of kanamycin and 50 µL of a glucose tracer ([1,2-^{13}C], [1,6-^{13}C], or [4,5,6-^{13}C] glucose) in each well. Optical density measurements were taken periodically over the next 22 hours, with 150 µL samples from each well centrifuged, separated, and stored (in a -20^{o}C freezer) for subsequent analysis at each time point.

3.5 Analytical Methods

Cell growth was determined by measuring optical density at a wavelength of 600 nm (OD_{600}) with a spectrophotometer (Eppendorf BioPhotometer). Triplicate measurements were averaged and adjusted to the optical density of the pure medium (rich or minimal). Cell counts obtained by plating for all strains at various stages of growth were observed to be linear with respect to OD_{600} and similar for all strains. This affirmed that optical density could be used to accurately measure total cell density in solution, despite the metabolic conditions and unique genetic background of each co-culture.

3.5.1 Derivatization of Amino Acids

Extraction and tert-butyldimethylsilyl (TBDMS) derivatization of amino acids from biomass was performed prior to GC-MS analysis. 1 mL samples were collected at OD_{600} values of approximately 0.5 and 1.0. The samples were centrifuged for 5 minutes at 14,000 rpm and the supernatant separated from the cell pellet. The pellet was hydrolyzed with 500 µL of 6 N HCl overnight at 110^{o}C. Next, the samples were centrifuged at 14,000 rpm for 5 minutes to remove cell debris. The contents were then transferred to an Eppendorf tube and evaporated to dryness under airflow at 60^{o}C. The dried samples were dissolved in 50 µL of methylhydroxylamine/pyridine solution and

incubated for 90 min at 37°C. After centrifugation to remove cell debris, 50 µL of N-tert-Butyldimethlysilyl-N-methyltrifluoroacetamide (MTBSTFA) + 1% TBDMCS were added and reacted for 30 minutes at 60°C. The samples were centrifuged one last time to remove cell debris; the liquid transferred to a GC injection vial for analysis.

3.5.2 Amino Acid Plating Assay

Strains within a co-culture were differentiated with an agar plating assay. Three types of plates were developed: rich (LB) media plates, minimal (M9) media plates with glucose and amino acids that enabled a specific strain's growth (see Table 4.2.1), and minimal (M9) media plates with glucose and no amino acids which served as a control. 40 µL of kanamycin monosulfate (50 mg/mL) were added to each plate to prevent contamination. Co-cultures in the logarithmic growth phase (OD_{600} between 0.5 and 1.0) were sampled and diluted accordingly (see text for further details), 10 µL of the diluted cultures then transferred to each type of plate, spread, and incubated at 37°C for 3-5 days. Cell concentrations in the units of colony forming units (CFU)/mL-OD_{600} were determined after this time by multiplying the number of colonies on a specific plate by the dilution factor and dividing by the optical density of the culture at the time of dilution/plating. These values were then compared to the known concentration of *E. coli* in solution (~ 10^9 cells/mL-OD_{600}).

3.6 Gas Chromatography Mass Spectrometry

GC–MS analysis was performed on an Agilent 7890B GC system equipped with a DB-5MS capillary column (30 m, 0.25 mm i.d., 0.25 mm-phase thickness; Agilent J&W Scientific), connected to an Agilent 5977 A Mass Spectrometer operating under ionization by electron impact (EI) at 70 eV. GC–MS analysis of tert-

butyldimethylsilyl (TBDMS) derivatized proteinogenic amino acids was performed as described previously by Antoniewicz et al.[10] Labeling of glucose in the medium was confirmed by GC–MS analysis of the aldonitrile pentapropionate derivative of glucose. Mass isotopomer distributions were obtained by integration of ion chromatograms and corrected for natural isotope abundances.

3.7 Metabolic Flux Analysis

^{13}C-MFA was performed by fitting mass isotopomer distributions to developed metabolic models through the Metran software package, which is built upon the elementary metabolite units (EMU) framework.[9] The *E. coli* network model used for flux calculations of mono-cultures has been described previously by Leighty and Antoniewicz[11], and is given in Figure 4.4.1. The model includes all major metabolic pathways of central carbon metabolism such as glycolysis, the pentose phosphate pathway, and the tricarboxylic acid (TCA) cycle as well as lumped amino acid biosynthesis pathways and a lumped reaction for cell growth. In addition, the model accounts for the exchange of intracellular and atmospheric CO_2, and G-value parameters to describe fractional labeling of amino acids.[12]

---

[10] Antoniewicz, M.R., Kelleher, J.K., Stephanopoulos, G. (2007). Accurate assessment of amino acid mass isotopomer distributions for metabolic flux analysis. Analytical Chemistry. 79 (19), 7554-9.

[11] Leighty, R.W., Antoniewicz, M.R. (2013). Complete-MFA: complementary parallel labeling experiments technique for metabolic flux analysis. Metab. Eng. 20, 49–55.

[12] Leighty, R.W., Antoniewicz, M.R. (2012). Parallel labeling experiments with [U-13C] glucose validate E. coli metabolic network model for 13C metabolic flux analysis. Metab. Eng. 14, 533–541.

For ^{13}C-MFA of co-cultures, a novel method developed by Gebreselassie and Antoniewicz was utilized.[13] This framework, incorporated in the Metran package, allowed for the estimation of species-specific fluxes with no physical separation or genetic manipulation of cells. Metabolic network models were developed with two compartments, each representative of a separate species, and included a set of exchange "reactions" to simulate the sharing of metabolites between species – the underlying cause of any observed synergy within the studied co-cultures (see text for further details). Additionally, an f_1 parameter was defined to describe the fraction of species #1 in the co-culture.

Within Metran, metabolic fluxes were estimated through minimization of variance-weighted sum of squared residuals (SSRs) between experimental and simulated values. Starting with fluxes of random initial values, flux estimation was repeated at least ten times to find a global solution. At convergence, 95% confidence intervals were computed for all estimated fluxes by evaluating the sensitivity of the minimized SSR to flux variations.[14]

---

[13] Gebreselassie, N.A., Antoniewicz, M.R. (2015). (13)C-metabolic flux analysis of co-cultures: a novel approach. Metab. Eng. 31, 132-139.

[14] Antoniewicz, M.R., Kelleher, J.K., Stephanopoulos, G. (2006). Determination of confidence intervals of metabolic fluxes estimated from stable isotope measurements. Metab. Eng. 8, 324–337.

Chapter 4

RESULTS AND DISCUSSION

4.1 Cooperative Strains

We began by selecting 11 strains of auxotrophic *E. coli* mutants from the Keio collection that demonstrated synergistic behavior in the study by Wintermute and Silver.[4] Each mutant strain contains a single gene deletion, preventing the biosynthesis of a metabolite essential for its growth. Supplementing strains with an external supply of the missing metabolite in solution, thus, promotes successful growth. Frozen stock of each mutant strain was used to inoculate mono-cultures of rich (LB) media, which were grown overnight. 100 μL of each mono-culture were then taken and combined accordingly in fresh solutions of minimal media to generate 18 unique co-cultures with two mutants (Δicd, Δppc) serving as "base" strains. In addition, 100 μL of each grown strain were subcultured into mono-culture controls containing 5 mL of minimal media to validate their auxotrophic phenotype. Growth was measured over three days. The results of the initial mono-culture and co-culture experiments, which included two separate trials for reproducibility, are included in Appendix A.1. Six successful co-cultures consisting of five different, conditionally lethal auxotrophic *E. coli* strains were chosen to narrow the scope of the study, the growth profiles of these co-cultures and their relevant mono-culture controls are shown in Figure 4.1.1, below.

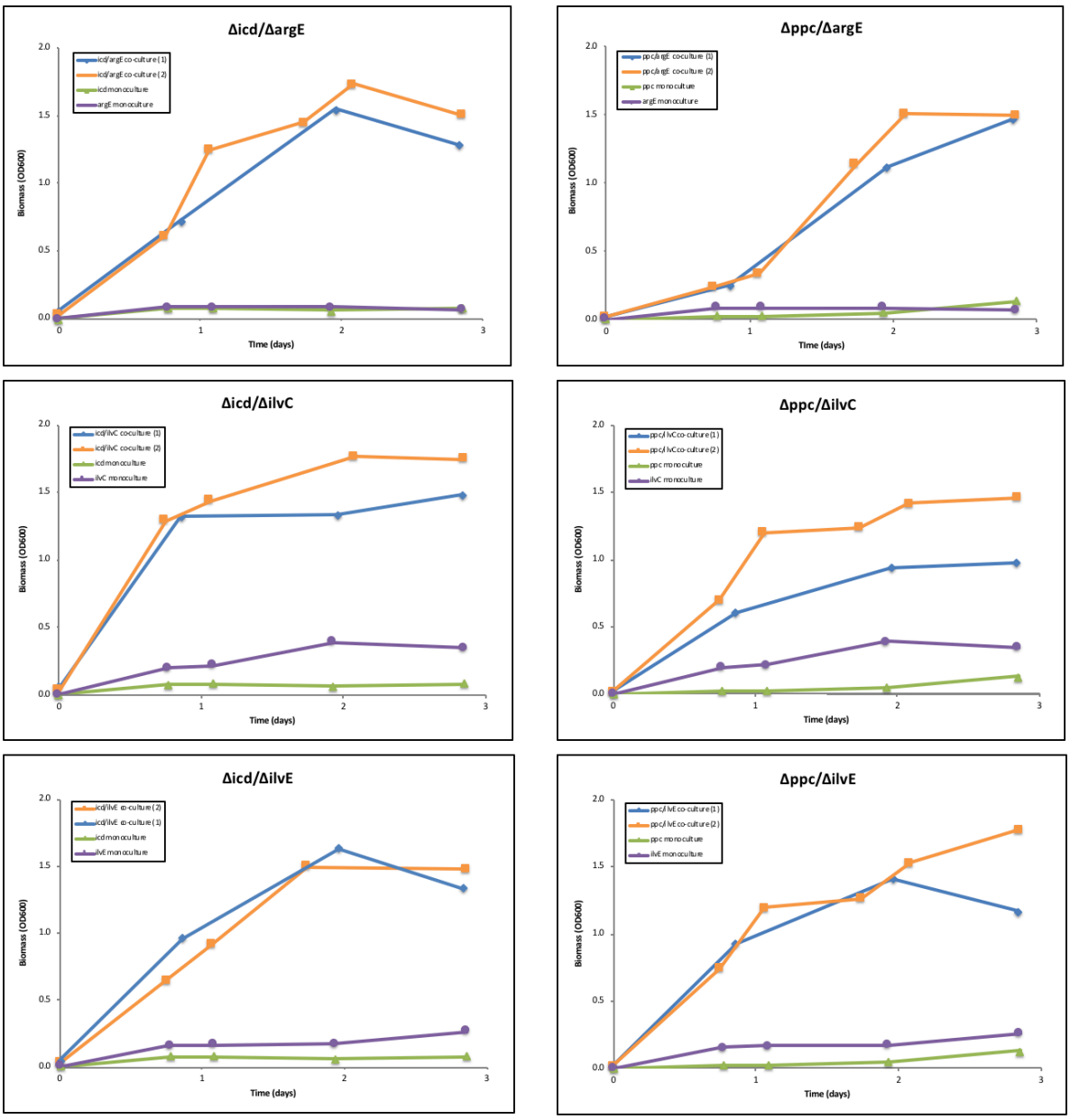

Figure 4.1.1. Synergistic growth in co-cultures of auxotrophic *E. coli* mutants in minimal media. Cultures of individual strains in minimal media included to show auxotrophic phenotype.

These results validate those of the 2010 study[1] while repeat trials demonstrate the reproducibility of observed mutualism between the involved species of specific co-cultures. The lack of growth observed in the control experiment (i.e. the *E. coli* mono-cultures) confirmed that we were indeed observing emergent cooperation between strains within a co-culture as well as reaffirmed that the strains were exhibiting an auxotrophic phenotype in minimal media.

4.2 Metabolic Restoration

To evaluate whether the acquired strains were auxotrophic due to single-gene deletions that inhibited the biosynthesis of essential metabolites, additional experiments were conducted which involved supplementing minimal media with amino acids. This series of experiments served a dual purpose: (1) it provided confirmation that the observed auxotrophy of the *E. coli* mutants was indeed caused by the genetic disruption of specific metabolic pathways and (2) it allowed us to differentiate between strains within a co-culture in future experiments by identifying the amino acids that recover metabolic function and, thus, promote cell growth in mono-cultures. Amino acids were selected for supplementation based on the product of the deleted gene in each *E. coli* mutant. Isocitrate dehydrogenase (ICDH), the icd gene product, plays a key enzymatic role in the TCA cycle, specifically, the reaction of isocitrate to α-ketoglutarate and CO_2. In addition, ICDH is utilized at the branch point between the citric acid and glyoxylate cycles to regulate carbon flux. We reasoned that the provision of glutamate to the Δicd mutant in minimal media would restore function of the TCA cycle and enable growth due to the reversibility of the glutamate biosynthesis reaction (wherein α-ketoglutarate serves as a reactant). Aspartate was included in responses to studies which demonstrate the difficulty of

wild-type (WT) *E. coli* strains to utilize glutamate as a substrate. For convenience, Figure B.1 is provided in the appendix and outlines the relationships between metabolites involved in central carbon metabolism and amino acid biosynthesis pathways of *E. coli*. Similar reasoning was followed in identifying aspartate and glutamate as the amino acids that would restore metabolic function to the Δppc knockout since its gene product, phosphoenolpyruvate carboxylase, produces oxaloacetate: a key intermediate of the TCA cycle and the precursor for the aspartate family of amino acids. To note, the fact that the same amino acids enable growth in both Δicd and Δppc did not introduce a problem into our study since both mutants were selected initially as "base" strains and never co-cultured together. This decision was made, in large part, because of the similarities between each knockout's gene product in terms of metabolic function. Similarly, arginine was identified as an appropriate supplement for the ΔargE mutant strain due to acetylornithine deacetylase's, the argE gene product, involvement in the first step of a biosynthesis subpathway incorporated into the metabolic pathway that produces L-arginine. Finally, isoleucine and valine were identified as the appropriate amino acid supplements for the ΔilvC mutant as ketol-acid reductoisomerase, the protein produced by the ilvC gene, participates in the second steps of two biosynthesis subpathways that produce L-isoleucine from 2-oxobutanoate and L-valine from pyruvate. Similarly, isoleucine and valine were identified as appropriate amino acid supplements for the ΔilvE mutant since the ilvE gene codes for branched-chain-amino-acid aminotransferase, an enzyme involved in step 4 of the biosynthesis subpathways that produce L-isoleucine from 2-oxobutanoate, L-leucine from 3-methyl-2-oxobutanoate, and L-valine from pyruvate. The observation that identical supplements

promote growth in both the ΔilvC and ΔilvE knockouts was anticipated based on the similarities in function of the two gene products. Complications arising from these findings were avoided in future experiments by ensuring both strains were never co-cultured together – another reason why Δicd and Δppc were identified as base strains for the experiments. In fact, as shown by Wintermute and Silver (2010), a co-culture containing ΔilvE and ΔilvC mutant strains is unable to grow in minimal media due to the overlapping function of each mutant's knocked-out metabolite.

Mono-cultures of each strain in minimal media supplemented with the amino acids listed in Table 4.2.1 were created and measured by optical density over an eight hour period. The observed growth confirmed that the respective amino acid supplements served as viable substitutes to each strains disrupted metabolic pathway. In addition, each strain was inoculated into mono-cultures of minimal media containing the incorrect amino acid supplement(s). The lack of growth observed in these cultures (see Appendix A.2), once again, confirmed the auxotrophic phenotype of the mutants while ensuring that the added amino acids support unrelated metabolic pathways in each strain. With these findings, we could now confidently and completely differentiate between strains of *E. coli* within experimental co-cultures based on which amino acids promote growth in subsequent analyses.

Table 4.2.1. Growth-enabling amino acid supplements for *E. coli* auxotrophs.

E. coli KO	*Supplemental Amino Acid(s)*	*Expt. Growth Rate in Minimal Media (h^{-1})*	*Expt. Growth Rate in Supplemented Media (h^{-1})*
Δicd	aspartate & glutamate	0.00	0.49
Δppc	aspartate & glutamate	0.03	0.43
ΔargE	arginine	0.00	0.55
ΔilvC	isoleucine and valine	0.01	0.54
ΔilvE	isoleucine and valine	0.01	0.52

4.3 Population Dynamics

So far, the aforementioned experiments confirmed our acquisition of conditionally lethal *E. coli* mutants, identified amino acid supplements that restore metabolic function to mono-cultures of auxotrophic mutants and, to the best of our knowledge, demonstrated emergent cooperation between strains within specific co-cultures. To check the latter and confirm that each co-culture was, in fact, demonstrating growth due to synergistic interactions between strains (as opposed to, say, the growth of a contaminating species), fresh Δicd/ΔargE and Δicd/ΔilvC co-cultures were inoculated and grown to stationary phase, then diluted 62,500x (250^2) and spread on both LB agar plates and amino acid supplemented M9 agar plates (hereby referred to as "selective plates"). After 48 hours of incubation, the plates were photographed and any visible cell colonies were counted – the results tabulated below.

Table 4.3.1. Colony counts on selective agar plates spread with diluted co-cultures after 48 hours of incubation.

Co-culture	*Plate Medium*			
	Rich (LB)	Minimal (M9) w/ aspartate, glutamate	Minimal (M9) w/ isoleucine, valine	Minimal (M9) w/ arginine
*Δ*icd/*Δ*argE	160	87	-	73
*Δ*icd/*Δ*ilvC	158	76	82	-

Here, the number of colonies are proportional to the concentrations of cells within each co-culture. Colonies present on the selective plates indicate the presence of individual strains (Δicd, ΔargE, or ΔilvC in this experiment). Since the relationship between colonies and cell concentration is linear, the sum of colonies present on the selective plates is expected to be near the number of colonies present on the rich (LB) agar plate if no contamination has occurred. Coincidentally, these summations result

in the exact number of colonies counted on each LB plate, suggesting that no contamination occurred within either co-culture. Furthermore, the near 1:1 ratios of colonies on the selective plates of each co-culture indicate that roughly an equal numbers of cells from each mutant strain were present in solution. These findings are consistent with those obtained by Wintermute and Silver (2010), supporting a metabolite exchange mechanism of *invested benefits*[15,16] in which the cooperation of one strain not only promotes growth in the other but augments its own as well. In other words, strain 1 is "motivated" to produce shared metabolites as it continues to receive benefits (shared metabolites) from strain 2. Assuming shared metabolites hold equal metabolic value to their recipients, we therefore expect and observed that successful co-cultures of auxotrophic *E. coli* contain near equal populations of individual strains. Here, the exchange network serves as an inherent control system in which overproduction of shared metabolites by either strain is immediately balanced out by the other strain's augmented growth. Eventually, we expect a limit to these invested benefits based on the availability of excess nutrients in solution (see Section 4.6). However, within these limits, the production of shared metabolites appeared to have no significant metabolic consequence on individual strains based on the observed growth rates of each co-culture.

---

[15] Connor, R.C. (1995). The benefits of mutualism: a conceptual framework. Biol. Rev. 70, 427–457.

[16] West, S.A., Griffin, A.S., Gardner, A. (2007). Social semantics: altruism, cooperation, mutualism, strong reciprocity and group selection. J. Evol. Biol. 20, 415–432

Two additional experiments were conducted to further test whether the synergistic interactions leading to cooperative growth of lethally conditional *E. coli* mutants in specific co-cultures follow the model of invested benefits. Δicd, ΔargE, and ΔilvC mutant strains were grown to stationary phase in mono-cultures of minimal media supplemented with the appropriate amino acids. Δicd/ΔargE and Δicd/ΔilvC co-cultures containing specific strain ratios at inoculation were then generated by measuring the optical density of each monoculture and aliquoting specific volumes as inoculum into fresh, minimal media. In total, six co-cultures were created, three containing Δicd and ΔargE strains and three containing Δicd and ΔilvC strains. The initial ratio of cells of each strain within the co-cultures were 20:80, 50:50, and 80:20. The co-cultures were observed over the next 51 hours. At four distinct time points, each co-culture was measured by optical density - a small sample of the cultures then diluted (62,500x) and spread on LB and selective agar plates. After an additional 48 hours, the plates were counted for cell colonies. The results of the Δicd/ΔargE co-cultures are shown in Tables 4.3, below, while the results of the Δicd/ΔilvC co-cultures are included in Appendix A.3.

Table 4.3.2. Results of ratio experiment for Δicd/ΔargE co-culture (80:20)

Time (hr)	*21.75*	*29.33*	*45.50*	*51.00*	***AVG (SD)***
OD600	0.292	1.704	1.647	1.632	-
M9 Plate w/ asp, glut [# of colonies]	14	142	139	124	-
M9 Plate w/ argE [# of colonies]	10	106	165	n/a	-
Sum	24	248	304	n/a	-
LB Plate [# of colonies]	49	208	244	203	-
Δicd Percentage	58%	57%	46%	61%*	56% (7)
ΔargE Percentage	42%	43%	54%	39%*	44% (7)
Cell Concentration [10^9 Cells/mL-OD600]	1.0	0.8	0.9	0.8	0.9 (0.1)

Table 4.3.3. Results of ratio experiment for Δicd/ΔargE co-culture (50:50)

Time (hr)	*21.75*	*29.33*	*45.50*	*51.00*	***AVG (SD)***
OD600	0.804	1.806	1.645	1.636	-
M9 Plate w/ asp, glut [# of colonies]	34	114	101	106	-
M9 Plate w/ argE [# of colonies]	53	155	165	n/a	-
Sum	87	269	266	n/a	-
LB Plate [# of colonies]	89	250	198	209	-
Δicd Percentage	39%	42%	38%	51%	43% (6)
ΔargE Percentage	61%	58%	62%	49%	57% (6)
Cell Concentration [10^9 Cells/mL-OD600]	0.7	0.9	0.8	0.8	0.8 (0.1)

Table 4.3.4. Results of ratio experiment for Δicd/ΔargE co-culture (20:80)

Time (hr)	*21.75*	*29.33*	*45.50*	*51.00*	***AVG (SD)***
OD600	0.614	1.754	1.624	1.590	-
M9 Plate w/ asp, glut [# of colonies]	37	104	129	74	-
M9 Plate w/ argE [# of colonies]	54	171	141	n/a	-
Sum	91	275	270	n/a	-
LB Plate [# of colonies]	73	245	229	208	-
Δicd Percentage	41%	38%	48%	36%	40% (5)
ΔargE Percentage	59%	62%	52%	64%	60% (5)
Cell Concentration [10^9 Cells/mL-OD600]	0.7	0.9	0.9	0.8	0.8 (0.1)

The total cell concentration in each co-culture across time points during which the cells were plated is consistent with the accepted value of $0.8*10^9$ cells/mL-OD600 for wild-type *E. coli*. It is important to note that ΔargE colonies could not be counted for each co-culture at the last time point (51 hours) due to a shortage of selective plates. Therefore, Δicd and ΔargE percentages were calculated at this interval using the number of colonies recorded for the LB plate. This calculation assumes no contamination has occurred within each culture, which is consistent with the observations at previous time points. Despite varied inoculum ratios, each individual population of cells within the Δicd/ΔargE co-culture equilibrated near 50% of the total cell population, as expected. Furthermore, equilibrium occurred quite rapidly in each co-culture as the initial, inoculum ratios of cells are undetectable (through colony counts) within one day of inoculation - even as optical density measurements indicate

the cultures are within the exponential phase of growth. This implies that strains within a co-culture are utilizing a very fast and/or efficient metabolite exchange mechanism, a hypothesis which is explored further in Section 4.6.

4.4 Preliminary Metabolic Flux Analysis of *E. coli* Co-cultures

4.4.1 Monocultures of *E. coli* Auxotrophs

Δicd/ΔargE and Δicd/ΔilvC co-cultures were selected for a preliminary ^{13}C metabolic flux analysis experiment. First, tracer experiments utilizing [1,2] and [1,6]-^{13}C glucose were performed on mono-cultures of the three individual strains (supplemented with amino acids). These results were then applied separately to a mono-culture network model for WT *E. coli* grown on glucose through the Metran software package. The metabolic network model was developed by Antoniewicz et al.[17] and is based on information provided by the KEGG database as well as experimental data. Included in the reaction network are all central carbon metabolism pathways, amino acid biosynthesis, and a lumped reaction for biomass accumulation. Optimization of flux fits for each dataset proceeded by minimization of sum-of-square residuals. Statistically acceptable fits (within a 95% confidence interval) were obtained for all experiments, the results displayed below as flux profiles. For comparison, a flux map of wild-type *E. coli* grown on glucose is provided. Fluxes are normalized against glucose uptake which has been set to a value of 100.

---

[17] Antoniewicz, M.R., Kraynie, D.F., Laffend, L.A., Gonzalez-Lergier, J., Kelleher, J.K., Stephanopoulos, G. (2007). Metabolic flux analysis in a nonstationary system: fed-batch fermentation of a high yielding strain of E. coli producing 1,3-propanediol, Metab. Eng., 9, 277–292

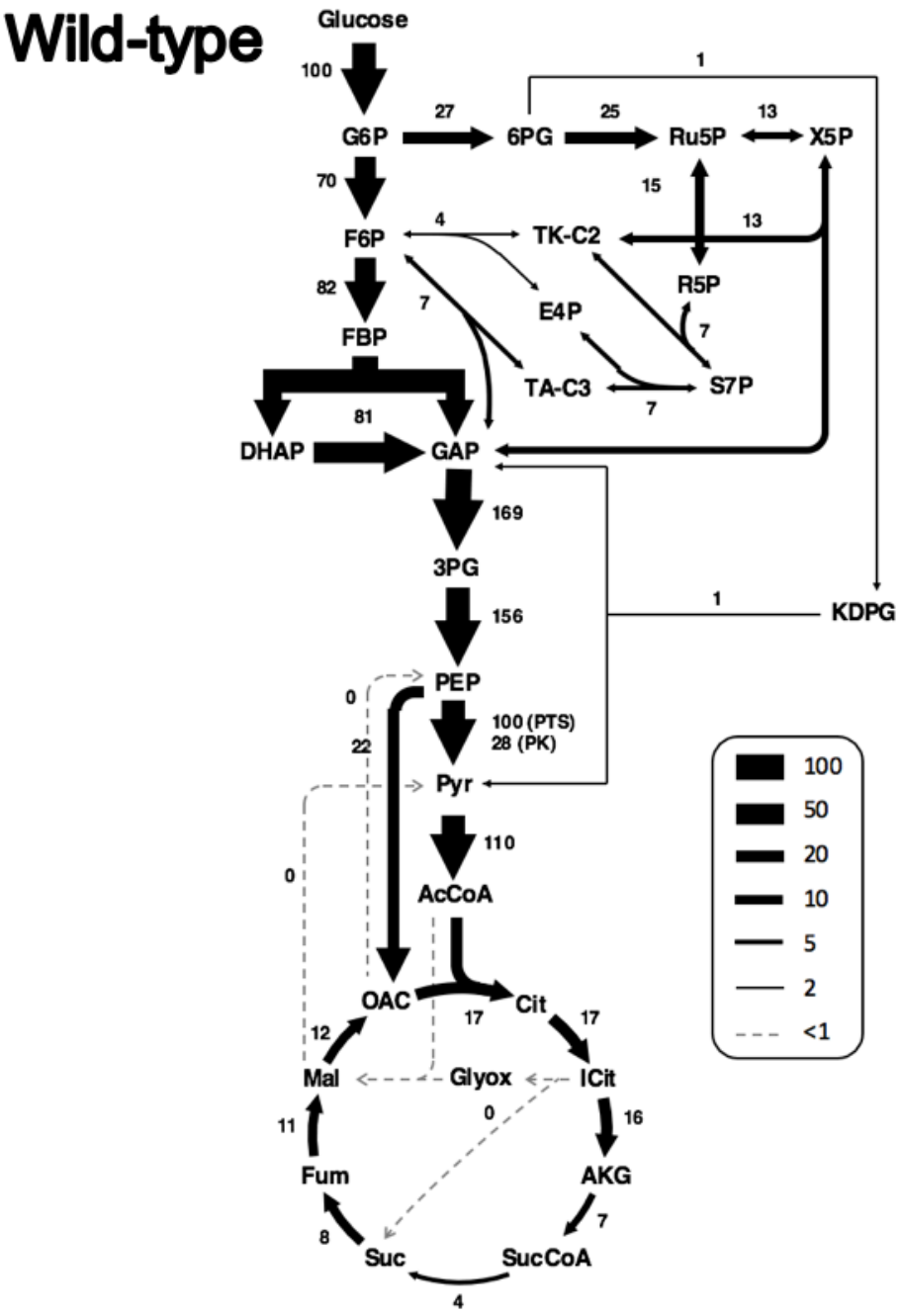

Figure 4.4.1. Metabolic flux profile of wild-type *E. coli* for growth on glucose

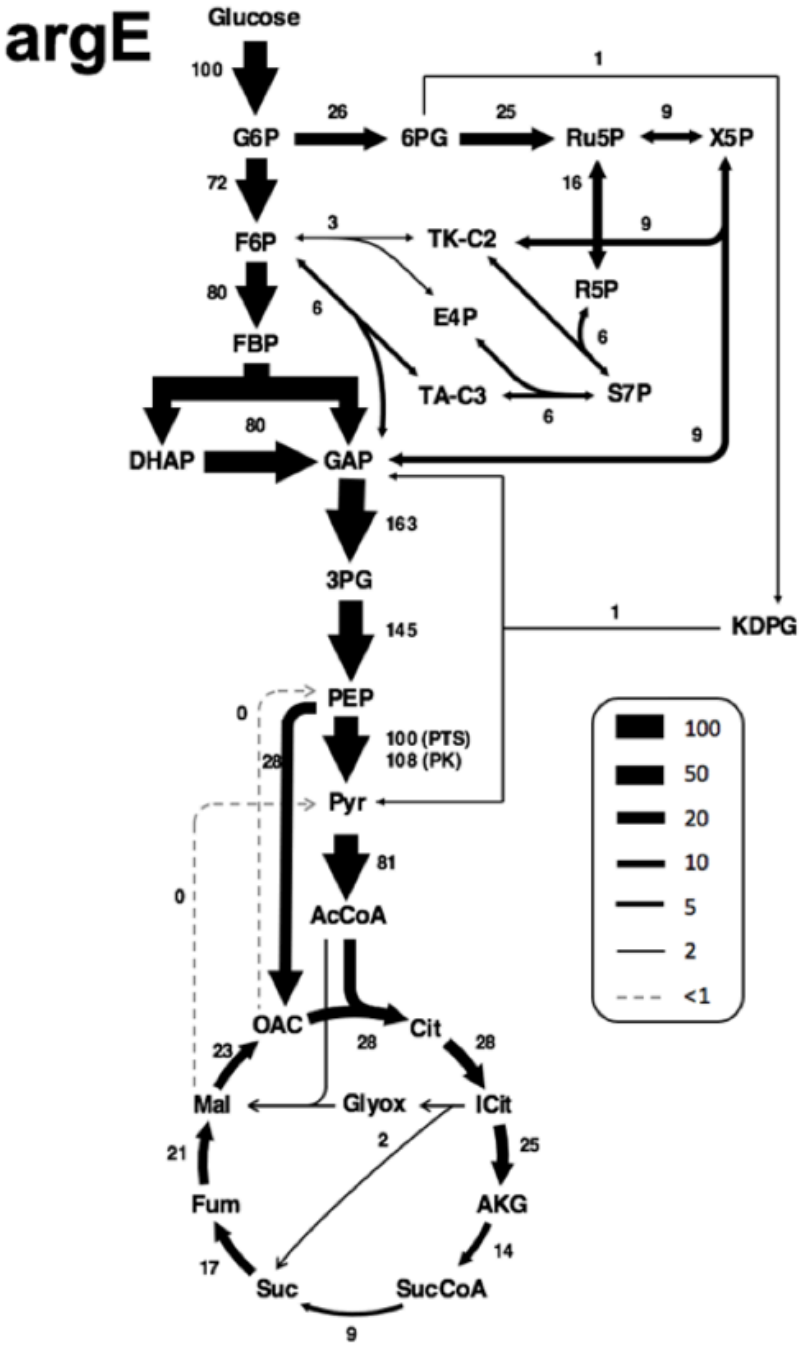

Figure 4.4.2. Metabolic flux profile of ΔargE mutant strain for growth on glucose

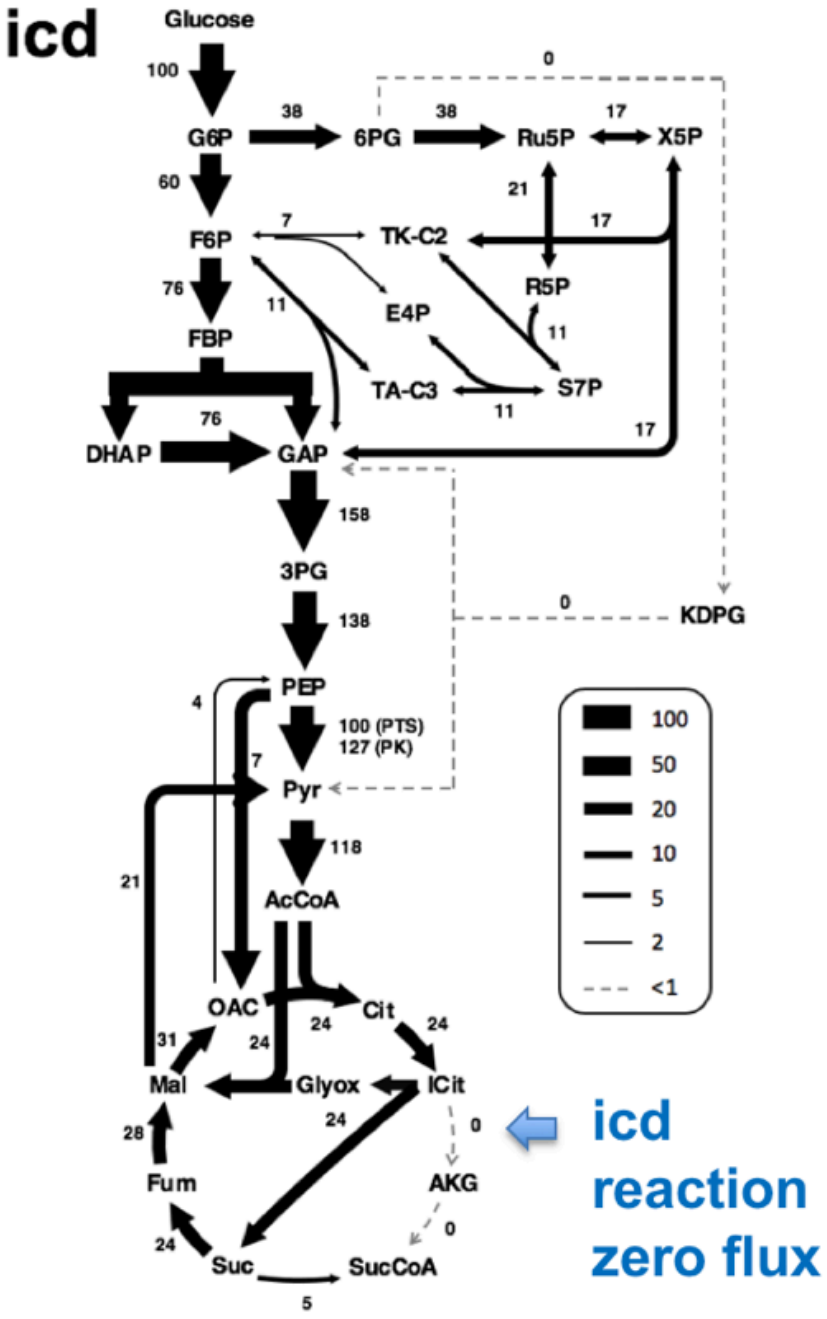

Figure 4.4.3. Metabolic flux profile of Δicd mutant strain for growth on glucose

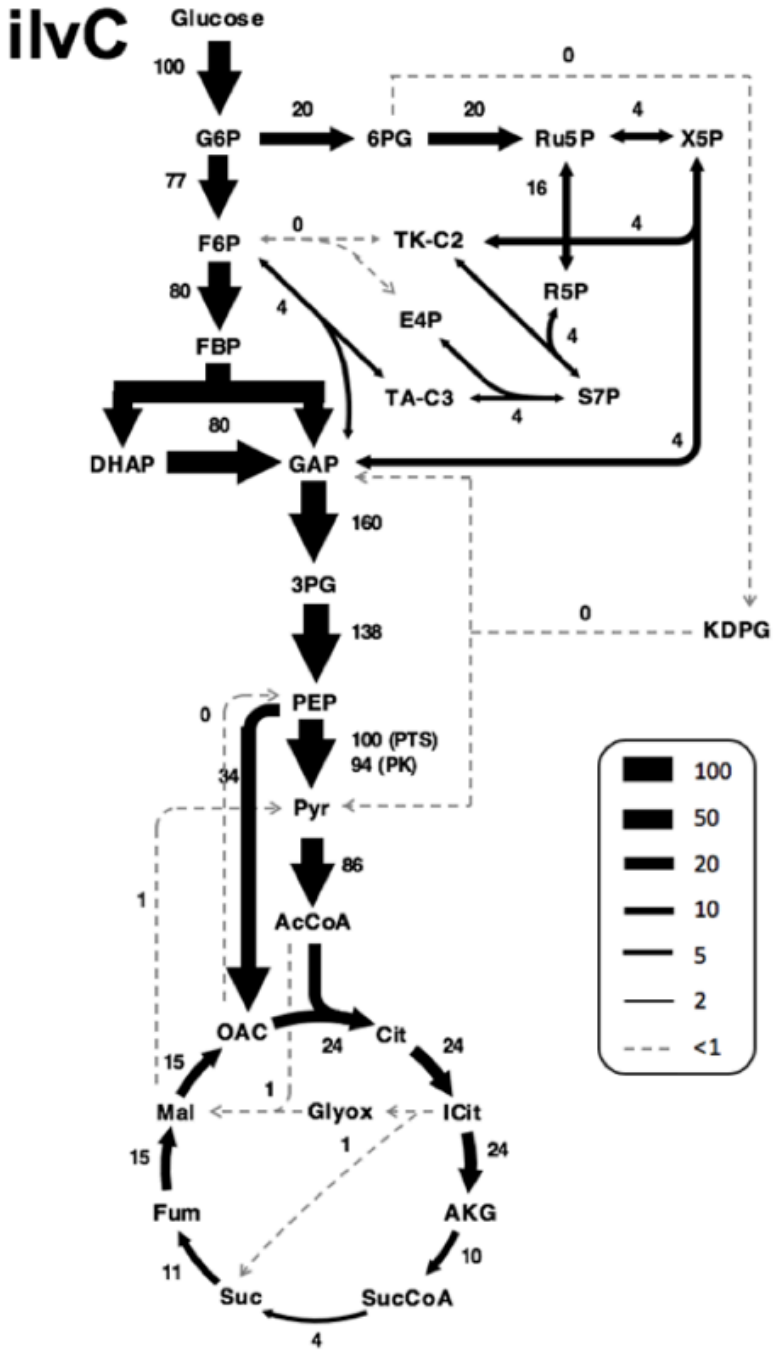

Figure 4.4.4 Metabolic flux profile of ΔilvC mutant strain for growth on glucose

As shown in Figures 4.4, glucose metabolism is characterized by high flux in upper glycolysis. All three mutant *E. coli* strains rely primarily on the Embden-Meyerhof-Parnas (EMP) and oxidative pentose phosphate (OPP) pathways for pyruvate production, exhibiting negligible flux through the Entner Doudoroff (ED) pathway. These results are consistent with those displayed by the native metabolism of the wild-type (WT) strain. The lack of flux between isocitrate and α-ketoglutarate (AKG) in the TCA cycle of Δicd's bioreaction network confirms the ablation of the icd gene by indicating an absence of isocitrate dehydrogenase. Reversely, the zero flux through this reaction validates the results of the metabolic model. To circumvent the disrupted pathway, activity in the glyoxylate pathway of Δicd's metabolism greatly increases. In doing so, the metabolic network bypasses the decarboxylation steps of the TCA cycle while continuing to provide energy and biosynthetic building blocks to the cell. Typically, the glyoxylate pathway is utilized for the breakdown of simple carbon compounds (such as acetate) when glucose is unavailable, however, Δicd can be seen here to take advantage of the secondary pathway out of necessity – enabling growth in minimal media supplemented with aspartate and glutamate. Here, the provided glutamate offsets the lack of AKG, obsoleting the first reaction in the amino acid biosynthesis network that produces glutamine, proline, histidine, and arginine.

Less distinct conclusions regarding changes in physiological state are drawn from the flux profiles of ΔargE and ΔilvC mutant strains. For both strains, flux through the TCA cycle is slightly increased over the metabolism of the WT *E. coli.* Generally, this increase can be attributed to a "backup" of specific metabolic pathways as each mutant strain is unable to catalyze a certain reaction within the amino acid biosynthesis pathway and must move matter elsewhere to maintain steady state.

4.4.2 Co-cultures of *E. coli* Auxotrophs

Metabolic flux analysis of co-cultures proceeded through a similar methodology. Upon completion of a tracer experiment involving the growth of co-cultures in minimal media with [1,2] and [1,6]-^{13}C glucose tracers, labeled mass fragment data from a subsequent GC-MS analysis was entered into Metran and fit to a mono-culture model to estimate metabolic fluxes. The obtained fits reveal the inability of the mono-culture model to accurately predict metabolic flux in species grown within a co-culture as the minimized sum of squares residuals (SSRs) lie significantly above the 95% confidence interval.

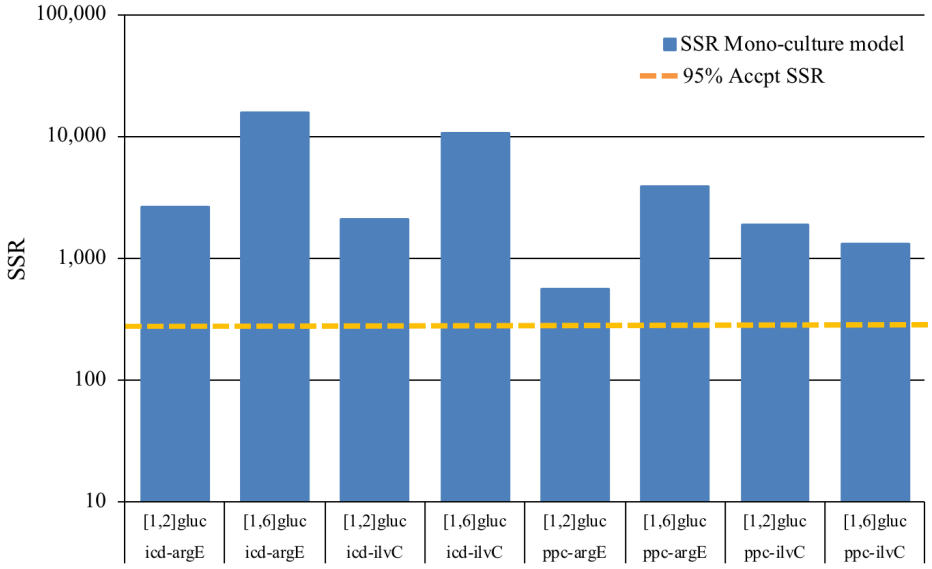

Figure 4.4.5. Minimized SSR values of best fits obtained using a mono-culture model for the ^{13}C-MFA of co-culture systems containing auxotrophic *E. coli* mutants, along with SSR values at 95% confidence level.

Next, co-culture models were developed to improve the accuracy of the flux estimates. These models included the mono-culture metabolic network for individual strains

(Figure 4.4.1, above) as well as exchange reactions that predict the metabolites shared between cell populations within each co-culture. Optimization proceeded by minimization of variance-weighted sum of squares residuals. Statistically acceptable fits (95% confidence) were obtained for Δicd/ΔargE and Δicd/ΔilvC co-cultures grown on [1,6]-^{13}C glucose (Appendix A.4). To note, the models developed through this preliminary metabolic flux analysis may be incomplete as they estimate exchange fluxes only for the metabolites most likely to be transferred within specific co-cultures. Thus, the metabolites discussed here may only represent a small collection of the total metabolites being transferred between strains.

4.4.2.1 Δicd/ΔargE Co-culture

For the Δicd/ΔargE co-culture, the optimized model included exchange reactions involving AKG and alanine – indicating these are the metabolites *most likely* being transferred between strains. Specifically, the flux estimates reveal Δicd uptakes AKG secreted by ΔargE while ΔargE uptakes alanine secreted by Δicd. The former exchange is as expected since the suppression of the Δicd gene prevents the production of ICDH and, thus, the catalysis of the isocitrate reaction within the TCA cycle. Therefore, ΔargE supplies the AKG required by Δicd in minimal media (no amino acid supplementation) to continue with central carbon metabolism and amino acid biosynthesis. Reversely, Δicd's provision of alanine to ΔargE was unanticipated. While the reaction of pyruvate into alanine is reversible, an increase in pyruvate flux into the TCA cycle was not observed within ΔargE's metabolism and would still not explain how the mutant circumvents the disrupted arginine biosynthesis subpathway which incorporates glutamate produced by AKG. Ultimately, the disconnect between arginine and alanine accentuates the gaps in the preliminary co-culture model.

4.4.2.2 Δicd/ΔilvC Co-culture

The flux results for the Δicd/ΔilvC co-culture indicate the exchange of AKG and isoleucine between strains. Once again, AKG flux points towards Δicd, indicating that ΔilvC supplies the metabolite to help Δicd overcome the lack of ICDH and disruption of the TCA cycle. Reversely, the model predicts isoleucine transfer from Δicd to ΔilvC. This exchange can be attributed to the lack of isoleucine production in ΔilvC caused by the absence of ketol-acid reductoisomerase. Since this enzyme is also involved in the production of L-valine from pyruvate, we are once again reminded of the incompleteness of this initial co-culture model.

4.5 Adaptive Laboratory Evolution Experiments

To examine whether the rate of transfer of metabolites between strains within individual co-cultures could be improved, a long-term adaptive laboratory evolution (ALE) experiment was conducted. ALE takes advantage of natural selection within large populations by continuously subjecting generations of cells to a controlled environment. By applying selective pressure, the fitness of each generation of microbe can be increased through mutagenesis. Δicd/ΔilvC and Δicd/ΔargE co-cultures were selected for this experiment and cultured sequentially over the course of several months. Periodically, the experiment was paused and the most current generation of cells were collected and stored in a -80^{o}C freezer. Co-cultures consisted of 10mL of minimal media, glucose, and 200μL of inoculum subcultured from the previous generation of cells upon reaching stationary phase. Overall, 38 generations of Δicd-ΔilvC and Δicd-ΔargE co-cultures were cultivated. Growth rates were measured at periodic generations to evaluate progress. The results of this experiment are shown in Table 4.5.1, below.

Table 4.5.1. Δicd/ΔargE and Δicd/ΔilvC growth rates across generations.

E. coli Co-Culture	*ALE # 1*	*ALE #22*	*ALE #38*
Δicd/ΔargE	0.170 h^{-1}	0.193 h^{-1}	0.265 h^{-1}
Δicd/ΔilvC	0.195 h^{-1}	0.237 h^{-1}	0.269 h^{-1}

After thirty-eight subcultures, both the Δicd/ΔargE and Δicd/ΔilvC co-cultures exhibited a significantly increased growth rate. These results indicate the development of a more efficient exchange mechanism between strains, through which evolved cells secrete and uptake metabolites at faster rates than the original mutants. Altogether, this experiment demonstrates the ability to improve the synergistic interactions between populations within specific co-cultures. A ^{13}C tracer experiment was conducted on the most current generation of co-cultures, the resulting supernatant and biomass stored at -80^{o}C. At the time of this work, a metabolic flux analysis was not conducted due to the lack of a complete and validated metabolic network model for *E. coli* co-cultures.

4.6 Metabolite Transfer Mechanism

Having identified a few of the key metabolites involved in the syntrophic exchanges between auxotrophic *E. coli* in specific co-cultures and demonstrated the ability to improve these exchanges through ALE, we next wanted to elucidate the details surrounding the physical mechanism through which cells were exchanging metabolites. Two hypotheses regarding the mechanism for cross feeding were considered: (1) cells secrete metabolites into solution, where they remain until uptaken by a cell of the opposite strain or (2) cells exchange metabolites through biomachinery built into their membranes, in which case two cells must come into contact for synergistic interaction to occur. To test which mechanism is enacted in vitro, Transwell® supports consisting of two wells (or, compartments) separated by a

semipermeable membrane were utilized. A procedure incorporating these supports was chosen over an experiment attempting to measure the concentrations of certain metabolites in solution since such methods have proven ineffective in deciphering syntrophic exchange mechanisms. This is due to the nature of the two proposed mechanisms, through which metabolites exist in solution at either such low concentrations or for such little time that accurate measurements are difficult to obtain. In addition, utilizing ^{13}C-MFA to analyze syntrophic interactions provides estimates of the *rates* of metabolite exchange. This is in contrast to experiments which are successful in measuring metabolite concentration in culture medium, as these values provides no insight on how fast exchange is occurring and, therefore, how important the metabolite is. By inoculating two adjacent wells containing minimal media and a glucose carbon source with a specific, conditionally lethal *E. coli* mutant and utilizing a semipermeable membrane (with pores large enough to allow for the transfer of small molecules but small enough to prevent cell transfer) as the shared wall between the two wells, we can create theoretical co-cultures of *E. coli* auxotrophs that directly test whether metabolites are exchanged through solution. If growth is observed in both wells (i.e. in each "pseudo" co-culture), the 1st proposed hypothesis is confirmed whereas no observed growth confirms the 2nd hypothesis.

Several preliminary trials of the procedure described above were conducted to validate the experimental methods before interpreting any results. First, it was concluded that the plates containing Transwell® supports would have to be shaken continuously in order to eliminate significant mass transfer limitations observed between wells. Since only a small surface area of the outer wells come into contact with air, cultures contained in these wells demonstrated significantly decreased growth

rates attributed to a lack of oxygenation. With shaking, it was then necessary to conduct experiments that evaluated whether contamination could occur between the inner and outer wells of a "co-culture" by spillage over the well walls. Ultimately, it was determined that an agitation rate of 200rpm would eliminate the oxygen transfer limitations between the air and outer wells without inducing any spillage.

Co-cultures consisting of Δicd and ΔilvC mutant strains were chosen for this analysis. Corning 3412 plates containing six separate sets of wells were used to generate six "co-cultures" simultaneously, each consisting of a well inoculated with Δicd (1:10 dilution) and a well inoculated with ΔilvC (1:10 dilution), separated by a semipermeable membrane. Strain placement was varied to test for differences in the inner and outer wells of a single support system. Cell growth was measured by optical density over 32 hours, the results displayed below. Green shading was added to help portray the relative growth in each well over time.

Table 4.6.1. OD_{600} of Δicd-ΔilvC co-cultures in Transwell permeable supports over time.

Culture #	Well Type	Strain	t = 0 hrs	t = 4 hrs	t = 8.75 hrs	t = 13.25 hrs	t = 24 hrs	t = 32 hrs
1	Inner Well	icd	0.061	0.123	0.218	0.409	1.546	1.441
	Outer Well	ilvC	0.086	0.172	0.263	0.443	0.475	0.489
3	Inner Well	icd	0.065	0.117	0.203	0.370	1.323	1.577
	Outer Well	ilvC	0.084	0.175	0.256	0.408	0.475	0.461
5	Inner Well	icd	0.064	0.124	0.209	0.370	1.146	0.778
	Outer Well	ilvC	0.086	0.177	0.252	0.432	0.574	0.624
2	Inner Well	ilvC	0.085	0.296	0.433	0.823	0.775	0.644
	Outer Well	icd	0.062	0.067	0.097	0.139	0.282	0.346
4	Inner Well	ilvC	0.085	0.333	0.439	0.759	0.685	0.692
	Outer Well	icd	0.063	0.068	0.093	0.132	0.266	0.333
6	Inner Well	ilvC	0.087	0.313	0.415	0.759	0.803	0.974
	Outer Well	icd	0.069	0.067	0.099	0.131	0.269	0.361

The observed growth confirms the employment of an exchange mechanism wherein cells secrete and uptake metabolites through a shared medium. Although cell contact is not required, rapid exchange (due, in part, to the proximity of cells) can result in extremely low concentrations of metabolites in solution – explaining the phenomenon in which researchers are unable to detect shared metabolites by measuring the medium. These findings are supported by the syntrophic exchange mechanism of *invested benefits*, discussed previously in Section 4.3. Qualitatively, this mechanism describes a competitive cooperation between strains within a co-culture through which cells are motivated to supply metabolites based on the benefits they receive in return. With this structure, any metabolite that is not immediately consumed by a cell of the opposite strain upon secretion signals to the secreting cell that the investment system has broken down and that it is no longer necessary to provide metabolites to receive benefits in return. Consequentially, to minimize metabolic burden, this strain may stop secreting the valued metabolite altogether. Ultimately, such a phenomenon would lead to an uneven distribution of cell populations, resulting in either a series of correction events to equilibrate the populations or, if left uncorrected, the monopolization and subsequent failure/death of the co-culture. To further demonstrate these population dynamics, the optical density measurements in Table 4.6.1, above, were compiled to show cell concentrations over time after adjusting for volumetric changes induced through periodic sampling. Figure 4.6.1, below, reveals each experimental co-culture (differed by their strain positions) trending towards an equal number of cells of each strain, thus, substantiating the predicted exchange mechanism.

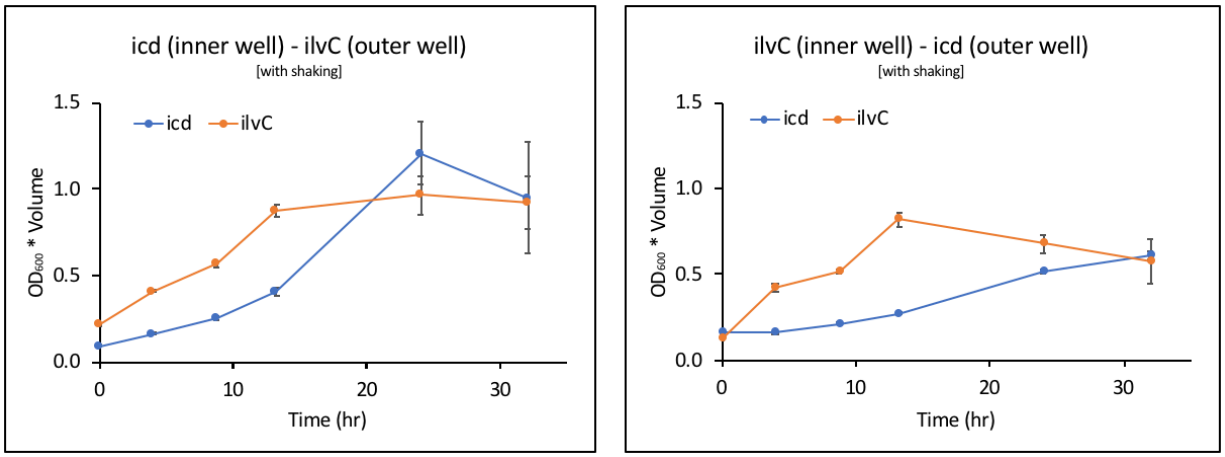

Figure 4.6.1. Number of cells (indicated by multiplying optical density by the volume of each culture at the time of sampling) over time in pseudo co-cultures consisting of Δicd and ΔilvC mutants in Transwell® permeable supports with strain position varied.

Assuming shared metabolites hold equal metabolic value to both *E. coli* strains, the equal number of cells between wells that make up each Δicd-ΔilvC (Transwell®) co-culture indicates uniform exchange of metabolites between strains. In other words, on average, each cell within a co-culture secretes the same amount of metabolites as it uptakes. Once again, these observations follow the model of *invested benefits*, as Figure 4.6.1 captures self-correcting population trends that lead to the eventual balancing of cell numbers over time. Furthermore, the position of each strain within the Transwell® co-culture systems (inner well vs. outer well) appears to have little impact on population results. In both scenarios, the ΔilvC mutant strain exhibits more aggressive initial growth until the lack of metabolites secreted from the slower-growing icd strain serves as a natural control mechanism which equilibrates the two populations. In fact, in Figure 4.6.1, an imbalance in metabolite exchange is observed

to quite rapidly equilibrate strain populations after icd overshoots the naturally imposed limit.

4.7 Complete Metabolic Flux Analysis of Δicd/ΔilvC Co-culture

An additional co-culture growth experiment in Transwell® permeable supports was conducted using ^{13}C labeled glucose tracers to acquire data for the metabolic flux analysis of Δicd/ΔilvC cultures. Each well was inoculated with the same initial cell count through a procedure outlined in Section 3.4.3. Six co-cultures were cultivated for this experiment in total, sets of two containing a specific glucose tracer ([1,2], [1,6], or [4,5,6]-^{13}C). Once again, the position of each strain (outer, well compartment or inner, Transwell® insert) was varied within the sets of co-cultures to test for any differences induced by the placement of the strains. Upon reaching steady state, the cell culture medium in each well (12 wells total) was plated on minimal and selective agar plates at 1:1 and 1:100 dilutions. The remaining solution in each well was then divided into 500μL samples, centrifuged, separated, and stored for subsequent analysis. Colony results from the agar plates after 72 hours of incubation validated the co-culture compositions (desired strains in correct wells with no contamination) and affirmed the correct strain placements.

The isotopomer data corresponding to each well of the Transwell® tracer experiment, acquired through GC-MS analysis of the collected biomass, was fit to a metabolic network model developed for mono-cultures of wild-type *E. coli* grown on glucose to establish the model's insufficiency. For 11 of the 12 wells, the SSR values corresponding to the best metabolic flux fits lie outside the acceptable range of 95% confidence (see Figure 4.7.1, below). These results confirm the inability of the mono-culture metabolic network model to accurately estimate fluxes for each pseudo co-

culture. These observations were anticipated, since the model fails to account for the cross-feeding of metabolites between strains, which ultimately drives co-culture growth.

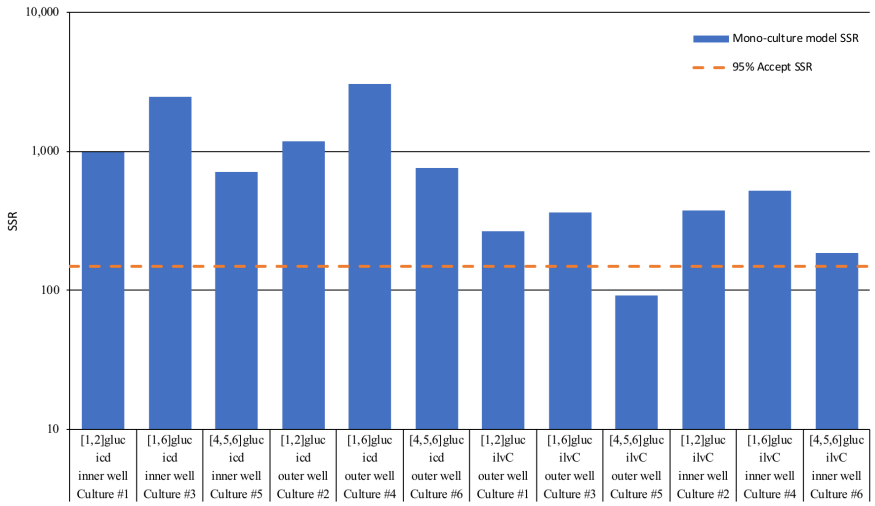

Figure 4.7.1. Minimized SSR values of best fits obtained using a mono-culture model for each compartment containing Δicd and ΔilvC strains for the ^{13}C-MFA of (pseudo) co-cultures in Transwell® semipermeable supports, along with threshold SSR values at 95% confidence level.

Once the *E. coli* mono-culture model was deemed inadequate, two separate co-culture models were developed to estimate metabolic fluxes for the Δicd/ΔilvC co-cultures. Each model contains two, separate metabolic networks following the template developed for a mono-culture of wild-type *E. coli* grown with glucose (see Figure 4.4.1) to capture the central metabolism of both the Δicd and ΔilvC strains, individually. In addition, each co-culture model contains a collection of exchange "reactions" that predicts the metabolites that are shared between strains. The collections of exchange reactions included in the two developed models represent two separate theories currently proposed in academia regarding the cross-feeding of

metabolites in microbial communities of *E. coli*.[7] The first model includes exchanges between amino acids synthesized by each strain while the second anticipates exchanges between intracellular organic acids such as malate, pyruvate, and citrate. Through one of these two models, we aim to capture all of the key metabolites exchanged between Δicd and ΔilvC mutant strains within a co-culture. In addition, a third co-culture model was developed which included all the exchange reactions encompassed by the original two models to test the possibility that an assortment of intracellular metabolites and amino acids contribute to the observed mutualism. The SSR values associated with the best fits for each co-culture system (inner and outer wells containing Δicd and ΔilvC mutant strains grown on a specific glucose tracer) are reported in Figure 4.7.2, below.

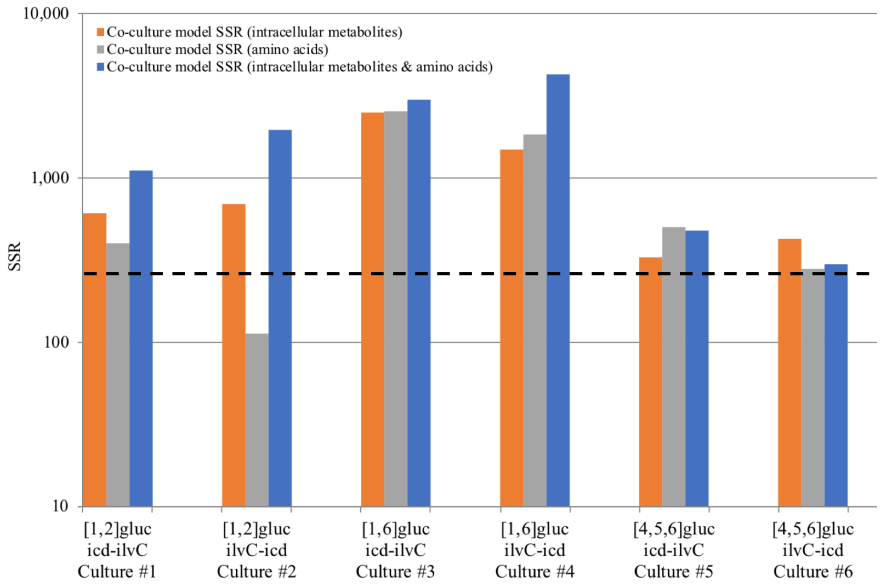

Figure 4.7.2. Results of ^{13}C-MFA using various co-culture models to estimate fluxes for co-culture systems of two *E. coli* knockouts (Δicd and ΔilvC) cultured on various ^{13}C glucose tracers in Transwell® permeable supports. Black line indicates threshold SSR values at 95% acceptable confidence level.

Small differences in the best-fit SSRs are observed across models for co-cultures grown on [1,6]-^{13}C and [4,5,6]-^{13}C glucose, respectively. In comparison, the MFA results show a significant decrease in the total SSR value reported for the amino acid exchange model fit to isotopomer data collected from Δicd/ΔilvC co-culture #2 (grown on [1,2]-^{13}C glucose). Since this value falls within the 95% acceptable confidence interval, the amino acid exchange model was selected for further analysis. Notably, the flux fits obtained by the combined co-culture model (which includes exchange reactions for amino acids *and* intracellular organic acids) report worse or near-equal SSRs compared to the other models across each Δicd/ΔilvC co-culture. This is likely due to overparameterization of the model, resulting in numerical instabilities that complicate the process of finding a global minimum.

In total, three datasets containing the isotopomer distributions of six separate wells (three tracers, two mutants, identical strain arrangement) were fit in parallel to the amino acid exchange model. The SSRs reported by the best fit (708.3) fell just outside the 95% acceptable confidence threshold (580). The flux estimates for this fit are reported in Figure 4.7.3, below. In addition to glutamate exchange (ΔilvC to Δicd), this model also predicts the exchange of serine (net flux = 16.5) from Δicd to ΔilvC. With further optimization, we believe this model can accurately estimate metabolic fluxes for the Δicd/ΔilvC co-culture.

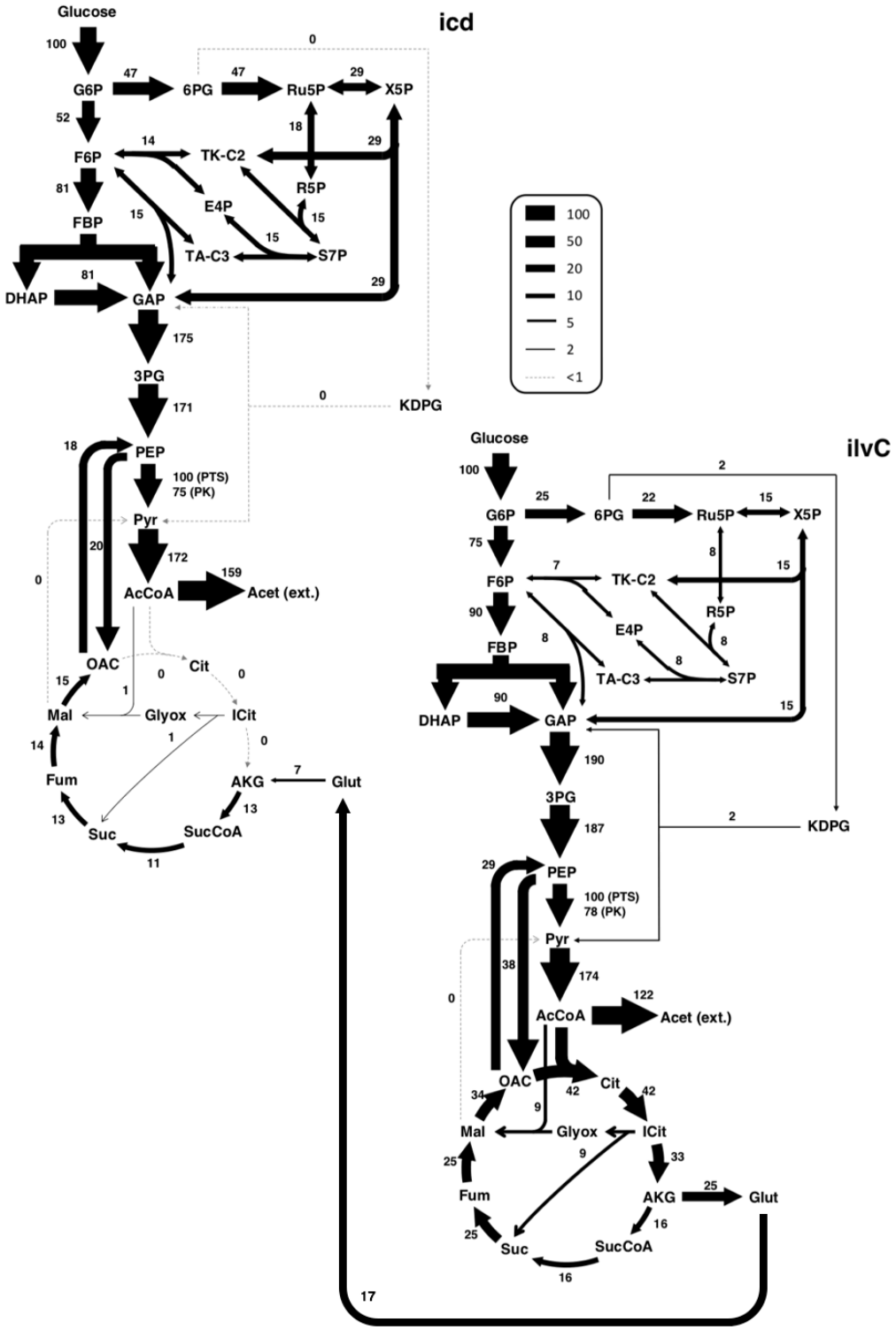

Figure 4.7.3. Metabolic flux profile of *E. coli* co-culture containing Δicd and ΔilvC mutant strains for growth on glucose.

Chapter 5

CONCLUSIONS

5.1 Conclusions

In this work, microbial communities consisting of two cooperative strains of auxotrophic *E. coli* were extensively studied to characterize the synergistic interactions between strains that enabled growth on glucose in minimal media. Eleven strains of lethally conditional *E. coli* mutants from the Keio collection were selected to generate 18 unique co-cultures, six of which were selected for further analysis due to the reproducibility of their growth results. By comparing the missing gene product of each mutant strain to known biochemical pathways comprising *E. coli*'s metabolism, amino acid supplements were identified and shown to promote mono-culture growth on glucose in otherwise minimal media. With these findings, experiments utilizing a selective plating assay and Transwell® permeable supports revealed self-limiting growth trends in cell populations within co-cultures. Here, it was shown that each strain acts as a negative feedback controller for the microbial system, efficiently exchanging metabolites through solution while following the mechanism of *invested benefits*. Adaptive laboratory evolution experiments demonstrated the ability to improve this exchange mechanism through mutagenesis inspired by the continuous application of selective pressures.

Mass isotopomer data and a mono-culture metabolic network model developed by Antoniewicz et al. (2012) were combined to accurately estimate central metabolism fluxes for mono-cultures of 4 mutant strains (Δicd, Δppc, ΔilvC, ΔargE) where disrupted pathways (i.e. reactions demonstrating zero flux) such as the conversion of isocitrate to AKG in the TCA cycle of Δicd validated the acquired strains. Next, this

network was used to develop co-culture models for the ^{13}C-MFA of a microbial community consisting of Δicd and ΔilvC mutant strains. Specific sets of exchange reactions were included in these models to test various hypotheses regarding metabolite exchange between strains. With data from a successful co-culture tracer experiment conducted within Transwell® permeable supports, a complete metabolic flux analysis was performed for each of the developed models – the results supporting an amino acid exchange model with reported SSRs (708.3) just outside the 95% confidence interval (530). The results of this model indicate the obligate exchange of glutamate and serine between Δicd and ΔilvC within a co-culture. With further tuning of the amino acid exchange model, we believe that accurate flux estimates can be obtained for the Δicd/ΔilvC co-culture as well as co-cultures of other cooperative pairs of conditionally lethal *E. coli*.

Overall, this report details the first extensive study of metabolite exchange within co-cultures of complementary *E. coli* auxotrophs that utilizes ^{13}C metabolic flux analysis. Insights gained by this work can go forth to benefit the optimization of microbial systems for industrial purposes (wastewater treatment, fermentation, etc.) as well as aid researchers in understanding certain biochemical phenotypes observed in nature.

5.2 Future Work

Throughout the course of this project, there were a few distinct points at which work was halted due to a shifting research focus. Therefore, there exists certain opportunities for the direct continuation of this work. In addition, many of the exciting concepts discussed in this work contain the potential to be explored and elaborated on

in future studies as our knowledge on synergistic interactions between microbial communities continues to expand.

As a near immediate continuation of the project, saved samples of the adaptively evolved co-cultures can be used to obtain isotopomer distributions through GC-MS analysis and fit through Metran to identify the metabolic changes contributing to the new physiological state of the co-cultures. Furthermore, ALE experiments involving these cultures can be renewed until a limit is observed with respect to improvements to the metabolite exchange mechanism (represented by growth rate). In addition, ^{13}C-MFA can be conducted on other co-cultures of *E. coli* auxotrophs to identify pattern amongst the exchanged metabolites. Of course, both these potential projects rely on the development of an accurate and generalized metabolic network model to describe cooperative co-cultures of auxotrophic *E. coli* which is the principal task. Again, this could be achieved by optimizing the amino acid exchange model developed in this work – identifying additional, relevant exchange reactions which fully and accurately fit isotopomer distributions.

In terms of pursuing broader research projects which further elucidate concepts discussed in this report, microbial communities consisting of only two microorganisms are also uncommon in nature, thus, the number of species studied within a given system can continue to be increased. As this number rises, the complexity of the metabolic interactions will increase as well and, therefore, so will the difficulty of the research in terms of identifying exchanged metabolites. In addition, studies which look to experimentally determine the same specie fluxes estimated by ^{13}C-MFA would be invaluable to the field as they can help validate and/or improve upon the current models and methods.

REFERENCES

1. Sabra, W., Dietz, D., Tjahjasari, D., Zeng, A.P. (2010). Biosystems analysis and engineering of microbial consortia for industrial biotechnology. Eng. Life Sci. 10, 407–421.

2. Bagi, Z., Acs, N., Bálint, B., Horváth, L., Dobó, K., Perei, K.R., Rákhely, G., Kovács, K.L. (2007). Biotechnological intensification of biogas production. Appl. Microbiol. Biotechnol. 76, 473–482.

3. Gilbert, E.S., Walker, A.W., Keasling, J.D. (2003). A constructed microbial consortium for biodegradation of the organophosphorus insecticide parathion. Appl. Microbiol. Biotechnol. 61, 77–81.

4. Wintermute, E.H., Silver, P.A. (2010). Emergent cooperation in microbial metabolism. Mol. Syst. Biol. 6, 407.

5. Gebreselassie, N.A., Antoniewicz, M.R. (2015). (13)C-metabolic flux analysis of co-cultures: A novel approach. Metab. Eng. 31, 132-139.

6. Baba, T., Ara, T., Hasegawa, M., Takai, Y., Okumura, Y., Baba, M., Datsenko, K.A., Tomita, M., Wanner, B.L., Mori, H. (2006). Construction of Escherichia coli K-12 in-frame, single-gene knockout mutants: the Keio collection. Mol. Syst. Biol. 2, 1-11.

7. Zengler, K., & Zaramela, L. S. (2018). The social network of microorganisms — how auxotrophies shape complex communities. *Nature Reviews Microbiology*.

8. Pande, S., et al. (2013) Fitness and stability of obligate cross-feeding interactions that emerge upon gene loss in bacteria. ISME J. 8, 953-962.

9. Antoniewicz, M.R., Kelleher, J.K., Stephanopoulos, G. (2007). Elementary metabolite units (EMU): a novel framework for modeling isotopic distributions. Metab. Eng. 9, 68–86.

10. Antoniewicz, M.R., Kelleher, J.K., Stephanopoulos, G. (2007). Accurate assessment of amino acid mass isotopomer distributions for metabolic flux analysis. Analytical Chemistry. 79 (19), 7554-9.

11. Leighty, R.W., Antoniewicz, M.R. (2013). Complete-MFA: complementary parallel labeling experiments technique for metabolic flux analysis. Metab. Eng. 20, 49–55.

12. Leighty, R.W., Antoniewicz, M.R. (2012). Parallel labeling experiments with [U-13C] glucose validate E. coli metabolic network model for 13C metabolic flux analysis. Metab. Eng. 14, 533–541.

13. Gebreselassie, N.A., Antoniewicz, M.R. (2015). (13)C-metabolic flux analysis of co-cultures: a novel approach. Metab. Eng. 31, 132-139.

14. Antoniewicz, M.R., Kelleher, J.K., Stephanopoulos, G. (2006). Determination of confidence intervals of metabolic fluxes estimated from stable isotope measurements. Metab. Eng. 8, 324–337.

15. Connor, R.C. (1995). The benefits of mutualism: a conceptual framework. Biol. Rev. 70, 427–457.

16. West, S.A., Griffin, A.S., Gardner, A. (2007). Social semantics: altruism, cooperation, mutualism, strong reciprocity and group selection. J. Evol. Biol. 20, 415–432

17. Antoniewicz, M.R., Kraynie, D.F., Laffend, L.A., Gonzalez-Lergier, J., Kelleher, J.K., Stephanopoulos, G. (2007). Metabolic flux analysis in a nonstationary system: fed-batch fermentation of a high yielding strain of E. coli producing 1,3-propanediol, Metab. Eng., 9, 277–292

Appendix A

Supplementary Data

A.1 Initial co-culture experiment: 18 pairs of *E. coli* auxotrophs

Table A.1.1. Trial 1 growth results (OD_{600} vs. time) for nine different co-cultures of auxotrophic *E. coli* from the Keio collection, using Δicd as a base strain

Time (days)	Base Strain: Δicd								
	+ ΔargE	+ ΔtrpE	+ ΔilvE	+ ΔilvC	+ ΔmetA	+ ΔcysC	+ ΔpanD	+ ΔnadC	+ ΔptsI
0.00	0.058	0.052	0.048	0.055	0.043	0.037	0.035	0.031	0.022
0.86	0.728	1.421	0.958	1.320	1.422	0.621	1.234	1.474	0.173
1.96	1.550	1.500	1.632	1.335	1.401	2.478	1.073	1.342	1.445
2.83	1.288	1.138	1.335	1.477	1.360	1.240	1.091	1.380	1.382
4.03	1.072	0.746	0.908	1.102	1.165	0.910	1.345	1.050	1.232

Table A.1.2. Trial 2 growth results (OD_{600} vs. time) for nine different co-cultures of auxotrophic *E. coli* from the Keio collection, using Δicd as a base strain

Time (days)	Base Strain: Δicd								
	+ ΔargE	+ ΔtrpE	+ ΔilvE	+ ΔilvC	+ ΔmetA	+ ΔcysC	+ ΔpanD	+ ΔnadC	+ ΔptsI
0.00	0.030	0.028	0.028	0.032	0.030	0.030	0.031	0.030	0.031
0.75	0.612	1.422	0.641	1.291	1.370	0.405	1.267	1.301	0.151
1.06	1.251	1.562	0.913	1.434	1.376	0.824	1.257	1.439	0.174
1.74	1.453	1.529	1.491	3.710	1.604	1.124	1.224	2.692	0.258
2.08	1.733	1.922	2.785	1.760	1.635	1.446	1.872	1.597	0.470
2.85	1.504	1.511	1.478	1.744	3.367	2.306	2.146	1.373	0.784

Table A.1.3. Trial 1 growth results (OD_{600} vs. time) for nine different co-cultures of auxotrophic *E. coli* from the Keio collection, using Δppc as a base strain

Time (days)	**Base Strain: Δppc**								
	+ ΔargE	**+ ΔtrpE**	**+ ΔilvE**	**+ ΔilvC**	**+ ΔmetA**	**+ ΔcysC**	**+ ΔpanD**	**+ ΔnadC**	**+ ΔptsI**
0.00	0.017	0.019	0.020	0.020	0.022	0.017	0.019	0.016	0.012
0.86	0.248	1.162	0.932	0.607	0.601	0.293	0.472	0.656	0.140
1.96	1.116	2.180	1.414	0.944	1.561	1.439	1.683	1.037	0.384
2.83	1.468	1.434	3.080	0.978	2.394	1.343	3.364	3.639	0.888
4.03	1.325	1.173	1.170	0.772	1.083	1.536	1.198	1.174	1.575

Table A.1.4. Trial 2 growth results (OD_{600} vs. time) for nine different co-cultures of auxotrophic *E. coli* from the Keio collection, using Δppc as a base strain

Time (days)	**Base Strain: Δppc**								
	+ ΔargE	**+ ΔtrpE**	**+ ΔilvE**	**+ ΔilvC**	**+ ΔmetA**	**+ ΔcysC**	**+ ΔpanD**	**+ ΔnadC**	**+ ΔptsI**
0.00	0.017	0.021	0.019	0.024	0.023	0.025	0.019	0.022	0.021
0.75	0.240	0.944	0.744	0.704	0.461	0.316	0.404	0.598	0.137
1.06	0.339	1.328	1.194	1.201	0.849	0.596	0.498	0.888	0.207
1.74	1.133	1.468	1.267	1.239	0.935	1.893	1.674	0.863	0.386
2.08	1.506	1.718	1.528	1.421	1.205	1.692	2.162	1.107	0.688
2.85	1.497	1.521	1.780	1.462	1.808	1.854	1.372	1.509	1.509

A.2 Amino acid supplementation experiment for *E. coli* mono-cultures

Table A.2.1. Growth Results (OD_{600} vs. time) for control experiment of mono-cultures of *E. coli* auxotrophs in minimal media.

Time (days)	Δicd	Δppc	ΔargE	ΔtrpE	ΔilvE	ΔilvC	ΔmetA	ΔcysC	ΔpanD	ΔnadC	ΔptsI
0.00	0.000	0.000	0.000	0.000	0.000	0.000	0.000	0.000	0.000	0.000	0.000
0.77	0.076	0.026	0.084	0.801	0.159	0.197	0.188	0.170	0.187	0.163	0.074
1.08	0.077	0.025	0.084	1.350	0.167	0.218	0.323	0.194	0.186	0.552	0.532
1.93	0.062	0.050	0.086	1.954	0.173	0.390	1.720	0.198	1.506	4.088	1.996
2.85	0.078	0.132	0.066	1.744	0.265	0.346	1.207	0.185	1.202	1.456	1.853

Table A.2.2. Growth Results (OD_{600} vs. time) for mono-cultures of *E. coli* auxotrophs in minimal media supplemented with specific amino acids.

Time (hr)	Δicd + asp + glut	Δppc + asp + glut	ΔilvE + ile + val	ΔilvC + ile + val	ΔargE + arg
0.00	0.068	0.078	0.095	0.092	0.100
0.92	0.086	0.097	0.141	0.139	0.130
2.00	0.142	0.165	0.263	0.251	0.226
2.92	0.231	0.239	0.412	0.407	0.391
4.00	0.384	0.366	0.714	0.735	0.545
5.17	0.566	0.497	1.186	1.253	0.612
5.83	0.605	0.521	1.449	1.531	0.662
6.83	0.647	0.576	1.868	1.975	0.744
8.50	0.739	0.687	2.058	2.117	0.921

Table A.2.3. Growth Results (OD_{600} vs. time) for mono-cultures of *E. coli* auxotrophs in minimal media supplemented with unrelated amino acids.

Time (hr)	Δicd + ile + val	Δicd + arg	Δppc + ile + val	Δppc + arg	ΔilvC + asp + glut	ΔilvE + asp + glut	Δarg + asp + glut
23	0.194	0.128	0.472	0.027	0.160	0.131	0.054

A.3 Ratio Experiment: Δicd/ΔilvC co-culture

Table A.3.1. Results of ratio experiment for Δicd/ΔilvC co-culture (80:20)

Time (hr)	*21.67*	*28.00*	*45.67*	*51.75*	***AVG (SD)***
OD600	0.127	0.517	0.981	1.498	-
M9 Plate w/ asp, glut [# of colonies]	3	18	71	72	-
M9 Plate w/ ile, val [# of colonies]	8	30	120	97	-
Sum	11	48	191	169	-
LB Plate [# of colonies]	14	52	120	147	-
Δicd Percentage	27%	38%	37%	49%	38% (9)
ΔilvC Percentage	73%	62%	63%	51%	62% (9)
Cell Concentration [10^9 Cells/mL-OD600]	0.7	0.6	0.8	0.6	0.7 (0.1)

Table A.3.2. Results of ratio experiment for Δicd/ΔilvC co-culture (50:50)

Time (hr)	*21.67*	*28.00*	*45.67*	*51.75*	***AVG (SD)***
OD600	0.320	1.145	1.453	1.466	-
M9 Plate w/ asp, glut [# of colonies]	27	37	96	110	-
M9 Plate w/ ile, val [# of colonies]	11	77	120	99	-
Sum	38	115	216	209	-
LB Plate [# of colonies]	36	90	174	150	-
Δicd Percentage	71%	32%	44%	73%	55% (20)
ΔilvC Percentage	29%	68%	56%	27%	45% (20)
Cell Concentration [10^9 Cells/mL-OD600]	0.7	0.5	0.7	0.6	0.6 (0.1)

Table A.3.3. Results of ratio experiment for Δicd/ΔilvC co-culture (20:80)

Time (hr)	*21.67*	*28.00*	*45.67*	*51.75*	***AVG (SD)***
OD600	0.473	1.170	1.360	1.433	-
M9 Plate w/ asp, glut [# of colonies]	25	55	119	101	-
M9 Plate w/ ile, val [# of colonies]	28	83	90	85	-
Sum	53	138	209	186	-
LB Plate [# of colonies]	45	114	150	150	-
Δicd Percentage	47%	40%	57%	43%	53% (12)
ΔilvC Percentage	53%	60%	43%	57%	47% (12)
Cell Concentration [10^9 Cells/mL-OD600]	0.6	0.6	0.7	0.7	0.6 (0.0)

A.4 ^{13}C-MFA results for preliminary model of Δicd/ΔargE and Δicd/ΔilvC co-cultures

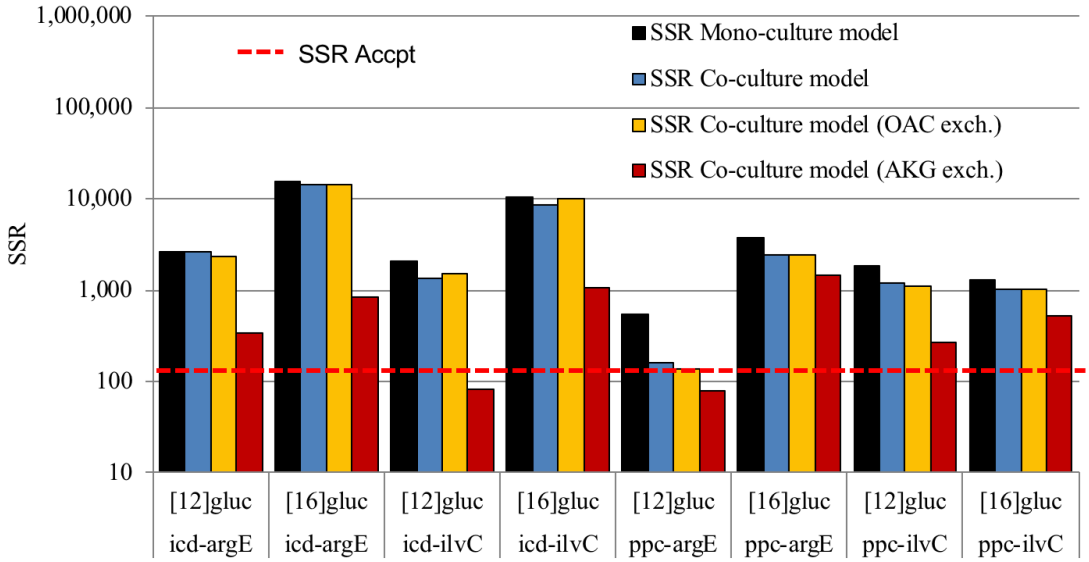

Figure A.4.1. Results of ^{13}C-MFA using simplified co-culture models to estimate fluxes for co-culture systems of two *E. coli* knockouts (Δicd/ΔargE and Δicd/ΔilvC) cultured on various ^{13}C glucose tracers. Red line indicates threshold SSR values at 95% acceptable confidence level.

A.5 Adaptive laboratory evolution experiments

Table A.5.1. Growth Results (OD_{600} vs. time) for ALE #22 of icd-argE co-culture in minimal media with glucose and kanamycin.

Time (hr)	8.78	10.53	12.20	13.45	14.20	15.20	16.53	17.70
icd-argE (ALE #22)	0.294	0.410	0.572	0.732	0.863	1.022	1.282	1.495

Table A.5.2. Growth Results (OD_{600} vs. time) for ALE #22 of icd-ilvC co-culture in minimal media with glucose and kanamycin.

Time (hr)	5.00	6.00	7.00	8.33	9.67	10.33	11.25	12.08	13.17	14.17
icd-ilvC (ALE #22)	0.111	0.132	0.164	0.221	0.313	0.371	0.476	0.600	0.765	0.954

Table A.5.3. Growth Results (OD_{600} vs. time) for ALE #38 of icd-argE co-culture in minimal media with glucose and kanamycin.

Time (hr)	0.00	1.75	3.42	5.67	7.33	9.42
icd-argE (ALE #38)	0.151	0.188	0.273	0.557	0.843	1.342

Table A.5.4. Growth Results (OD_{600} vs. time) for ALE #38 of icd-ilvC co-culture in minimal media with glucose and kanamycin.

Time (hr)	0.00	2.83	5.00	7.00	8.75	10.25	12.42
icd-ilvC (ALE #38)	0.093	0.120	0.162	0.257	0.440	0.635	1.172

A.6 Tracer experiment of Δicd/ΔilvC co-cultures in Transwell® Supports

Table A.6.1. OD_{600} of Δicd/ΔilvC co-cultures in Transwell® supports w/ various ^{13}C glucose tracers over 22 hours.

Culture	Position	Strain	Tracer	t = 0 hrs	t = 4 hrs	t = 9 hrs	t = 19 hrs	t = 22 hrs
1	Inner Well	Δicd (s4)	[1,2]	0.211	0.297	0.419	1.100	1.513
	Outer Well	ΔilvC (s4)	[1,2]	0.127	0.127	0.132	0.339	0.413
2	Inner Well	ΔilvC (s4)	[1,2]	0.217	0.327	0.411	1.430	1.893
	Outer Well	Δicd (s4)	[1,2]	0.124	0.144	0.200	0.381	0.505
3	Inner Well	Δicd (s4)	[1,6]	0.204	0.314	0.426	0.980	1.361
	Outer Well	ΔilvC (s4)	[1,6]	0.126	0.124	0.137	0.327	0.385
4	Inner Well	ΔilvC (s4)	[1,6]	0.213	0.347	0.416	1.239	1.792
	Outer Well	Δicd (s4)	[1,6]	0.125	0.140	0.204	0.372	0.508
5	Inner Well	Δicd (s4)	[4,5,6]	0.204	0.293	0.421	1.114	1.582
	Outer Well	ΔilvC (s4)	[4,5,6]	0.127	0.124	0.128	0.332	0.390
6	Inner Well	ΔilvC (s4)	[4,5,6]	0.214	0.354	0.423	1.297	1.768
	Outer Well	Δicd (s4)	[4,5,6]	0.123	0.152	0.226	0.402	0.567

Table A.6.2. Number of cells (OD_{600} *mL) in Δicd/ΔilvC co-cultures grown within Transwell® supports w/ various ^{13}C glucose tracers over 22 hours.

Culture	Position	Strain	Tracer	t = 0 hrs	t = 4 hrs	t = 9 hrs	t = 19 hrs	t = 22 hrs
1	Inner Well	Δicd (s4)	[1,2]	0.316	0.402	0.502	1.155	1.362
	Outer Well	ΔilvC (s4)	[1,2]	0.317	0.300	0.290	0.695	0.784
2	Inner Well	ΔilvC (s4)	[1,2]	0.325	0.442	0.494	1.502	1.704
	Outer Well	Δicd (s4)	[1,2]	0.310	0.339	0.439	0.780	0.960
3	Inner Well	Δicd (s4)	[1,6]	0.306	0.423	0.512	1.029	1.225
	Outer Well	ΔilvC (s4)	[1,6]	0.316	0.292	0.302	0.670	0.732
4	Inner Well	ΔilvC (s4)	[1,6]	0.319	0.468	0.499	1.301	1.613
	Outer Well	Δicd (s4)	[1,6]	0.313	0.329	0.448	0.763	0.965
5	Inner Well	Δicd (s4)	[4,5,6]	0.306	0.395	0.505	1.169	1.424
	Outer Well	ΔilvC (s4)	[4,5,6]	0.318	0.292	0.282	0.680	0.742
6	Inner Well	ΔilvC (s4)	[4,5,6]	0.321	0.478	0.507	1.362	1.591
	Outer Well	Δicd (s4)	[4,5,6]	0.308	0.358	0.498	0.824	1.078

Appendix B

Amino Acid Biosynthesis Pathways in *E. coli*

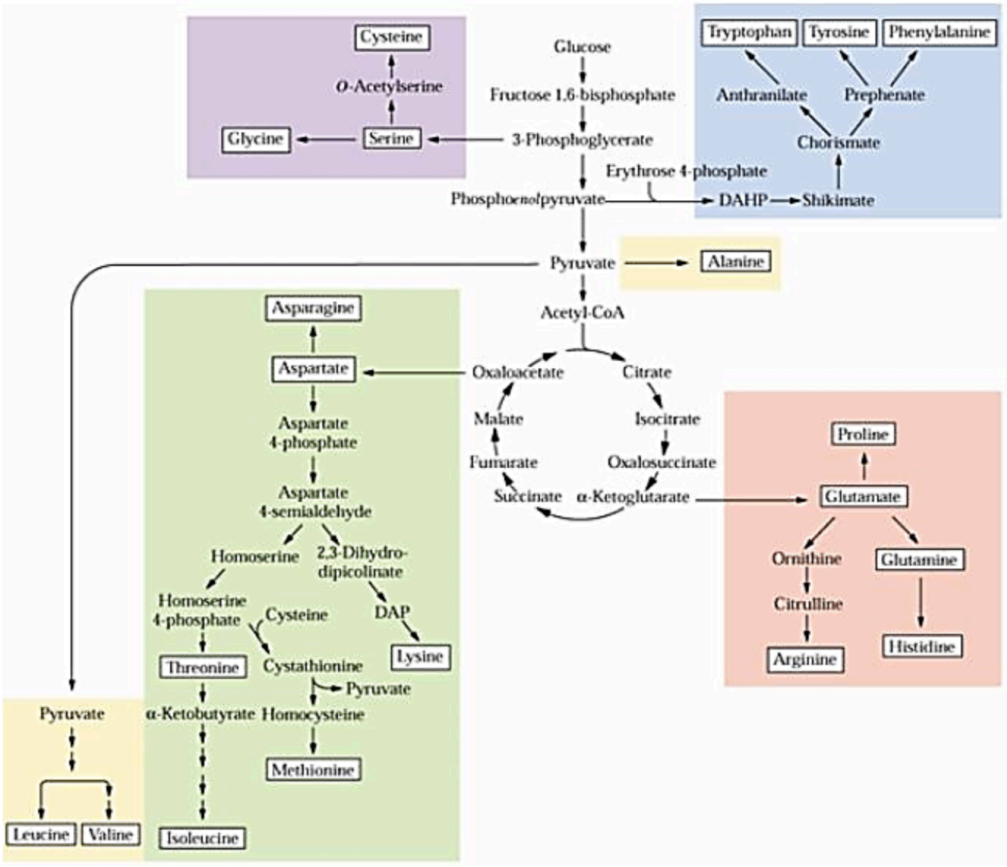

Figure B.1. Central carbon metabolism of *E. coli* and related amino acid biosynthesis pathways.